Thesis for the degree of Doctor of Philosophy
in the Natural Sciences

Signal Transduction in Photoreceptor Proteins

Insights From Time-Resolved X-ray Solution Scattering

Oskar Berntsson

UNIVERSITY OF GOTHENBURG

Department of Chemistry and Molecular Biology
Gothenburg, 2017

Thesis for the degree of Doctor of Philosophy
in the Natural Sciences

Signal Transduction in Photoreceptor Proteins
Insights From Time-Resolved X-ray Solution Scattering

Oskar Berntsson

Cover: A Light-Oxygen-Voltage photosensor domain on a 2D solution scattering pattern.

ISBN 978-91-629-0318-3 (Print)
ISBN 978-91-629-0319-0 (PDF)
Available online at http://hdl.handle.net/2077/53768

Department of Chemistry and Molecular Biology
Division of Biochemistry and Structural Biology
University of Gothenburg
SE-405 30, Göteborg, Sweden
Printed by BrandFactory AB
Göteborg, Sweden, 2017

Abstract

The ability to sense and react to different light conditions is of great importance for many organisms on the face of the earth. Specialized proteins known as photoreceptor proteins provide bacteria, plants and animals with this ability. To be able to sense the light the photoreceptor proteins have small molecules, known as chromophores, embedded within the protein matrix. Absorbed light triggers photochemical changes in the chromophore. These changes are relayed to the protein as structural changes and the biochemical activity of the protein is modified, thereby passing the signal on.

In this thesis, time-resolved X-ray solution scattering has been used together with molecular dynamics simulations to probe the conformational dynamics of photoreceptor proteins. The investigations reveal both the sequence and nature of light-induced structural transitions. Diverse mechanisms of signal transduction on different length- and timescales were found, from the nanometer scale light-induced separation of domains in phytochromes, to the Ångström scale opening of the light-oxygen-voltage dimer and subsequent supercoiling of the linker region, to the sub Ångström changes in the radius of gyration of cryptochromes. The results provide a structural link between the early photochemical events and the interaction and regulation of downstream processes and proteins.

Acknowledgements

The work towards a PhD is not a *one man show* and there are several people for whose support, both personal and professional, I am tremendously grateful.

I want to start by thanking my supervisor **Sebastian**, for taking me on as a student. Thank you for your support and that I could always come to you with questions. I am also very grateful for all the freedom you gave me to manage my own projects. I will not forget when you told me it was time to find a project of my own: "Find a protein for which there is a crystal structure available. Also, it should undergo a (substantial) light triggered conformational change, revert back to the dark state fast enough, be stable for hours and possible to prepare in high amounts". I read so many papers on photoreceptor proteins and finally found the light triggered histidine kinase YF1, with a recently solved structure.

This leads me to the second group of people without who I would not have been able to conduct this work, the collaborators. I have been fortunate to collaborate with people who have agreed to put in a significant number of working hours to prepare proteins for me to blast away at different beamtimes. So thank you **Janne** and **Heikki** for all the phytochromes, thank you **Andreas** and **Ralph** for all the LOV, and thank you **Erik** and **Ryan** for supplying cryptochrome samples.

I want to thank **Richard** for being my examiner; thank you for signing the important papers and for the yearly "So, how's Sebastian as a supervisor?" checkups.

A lot of this work was carried out during beamtimes at synchrotrons all over the world. This would not have been possible, and certainly not enjoyable without the people who traveled there with me: **Léo**, **Alex B**, **Ash**, **Matt**, **Stephan**, **Joachim**, **Maria** and **Emil**. Thank you for all the great *strahlzeits* and also for great *pre* and *post* beamtime vacations! The thanks also extend to the beamline staff at **BioCARS**, **cSAXS** and **ID09b**, who helped us set the experiments up, and who picked up the phone in the middle of the night to help when something had gone wrong.

I am also happy that I've gotten to know all the other great people of the Westenhoff group. **Petra E**, almost your turn now, I'm sure you will do great! **Elin C**, one of the most bitter and fun collegues, it was great fun going with you and Petra to Las Vegas. Thank you **Linnéa** for keeping people in order, and welcome to the group **Martin**.

I would probably not have started my PhD studies had I not first been part of the Katona group. Thank you **Anette** and **Gergely** for having me as a master student and thank you **Weixiao** for pointing me in their direction. It was a great year with lots of fun. Thank you also **Ida** for bringing me along to my first *proper* beamtime.

It's been a great few years in the Lundberg lab, and it wouldn't have been as fun without all the coffee breaks, beerclubs, crayfish and christmas parties, etc. So thank you **Rob D**, it was only business as I usurped the beerclub throne, **Petra B**, **Cecilia S**, **Daniel**, soon enough you'll be the WAXS-master, **Majo**, **Rebecka**, the lunch boxes are much less judged since you went on maternity leave, **Giorgia**, I can't wait to see what will happen if you manage to steal Rebecka's office space , **Elin D**, **Andreas**, **Cecilia W**, **Greger** & **Rajiv**, you guys make a terrific brain-smoothie, **Florian**, no one can prepare a tomato and mozzarella sandwich like you, **Viktor**, **Rhawnie**, **Maja**, **Rob B**, **Alex J**, **Davide**, **Dimitria**, **Stefan**, **Stanislav**, **Vijay**, **Kristina**, **Rosie**, **Gisela**, **Johanna**, **Björn**.

Also thanks to the Lundberg retirees: **David**, I have missed the presence of my live mirror since you left, **Mike**, **Jennie**, **Vlad** & **Billy**, it was great fun sharing the master student's office with you two.

Thank you **Bruno** and **Lars** for making sure that the computers and equipment (and Friday fika) are working.

To all the new people of the lab that I have yet to get to know more properly, welcome **Emelie**, **Darius**, **Swagatha**, and good luck with your projects/coffee breaks.

Jag vill också tacka mina **vänner och familj**. Jag hade uppenbarligen fel när jag som liten sa att forska, det skulle jag knappast göra.

Och sist men inte minst, tack så mycket **Anna**. Tack för att du stöttar mig, säger emot mig och framför allt, står ut med mig och mina resor. Jag älskar dig.

Publications

This thesis consists of the following research papers:

PAPER I: H. Takala*, A. Björling*, O. Berntsson, H. Lehtivuori, S. Niebling, M. Hoernke, I. Kosheleva, R. Henning, A. Menzel, J.A. Ihalainen, S. Westenhoff, "Signal amplification and transduction in phytochrome photosensors", *Nature* **509**, 245-248 (2014), doi: 10.1038/nature13310

PAPER II: A. Björling*, O. Berntsson*, H. Lehtivuori, H. Takala, A.J. Hughes, M. Panman, M. Hoernke, S. Niebling, L. Henry, R. Henning, I. Kosheleva, V. Chukharev, N.V. Tkachenko, A. Menzel, G. Newby, D. Khakhulin, M. Wulff, J.A. Ihalainen, S. Westenhoff, "Structural photoactivation of a full-length bacterial phytochrome", *Science Advances* **2**, e1600920-e1600920 (2016), doi: 10.1126/sciadv.1600920

PAPER III: O. Berntsson*, R.P. Diensthuber*, M.R. Panman, A. Björling, A.J. Hughes, L. Henry, S. Niebling, G. Newby, M. Liebi, A. Menzel, R. Henning, I. Kosheleva, A. Möglich, S. Westenhoff, "Time-resolved X-ray solution scattering reveals the structural photoactivation of a light-oxygen-voltage photoreceptor", *Structure (London, England : 1993)* **25**, 933-938.e3 (2017), doi: 10.1016/j.str.2017.04.006

PAPER IV: O. Berntsson*, R.P. Diensthuber*, M.R. Panman, A. Björling, E. Gustavsson, M. Hoernke, A.J. Hughes, L. Henry, S. Niebling, H. Takala, J.A. Ihalainen, G. Newby, S. Kerruth, J. Heberle, M. Liebi, A. Menzel, R. Henning, I. Kosheleva, A. Möglich, S. Westenhoff, "Sequential conformational transitions and α-helical supercoiling regulate a sensor histidine kinase", *Nature Communications* **8**, 284 (2017), doi: 10.1038/s41467-017-00300-5

PAPER V: O. Berntsson*, R. Rodriguez*, L. Henry, M.R. Panman, A.J. Hughes, J.A. Ihalainen, R. Henning, I. Kosheleva, E. Schleicher, S. Westenhoff, "Signal transduction in Drosophila melanogaster cryptochrome", *Manuscript*, (2017)

Related papers that I have co-authored but that are not included in this thesis:

PAPER VI: A. Björling, O. Berntsson, H. Takala, K.D. Gallagher, H. Patel, E. Gustavsson, R. St. Peter, Phu Duong, A. Nugent, F. Zhang, P. Berntsen, R. Appio, I. Rajkovic, H. Lehtivuori, M.R. Panman, M. Hoernke, S. Niebling, R. Harimoorthy, T. Lamparter, E.A. Stojković, J.A. Ihalainen, S. Westenhoff, "Ubiquitous structural signaling in bacterial phytochromes", *The Journal of Physical Chemistry Letters* **6**, 3379-3383 (2015), doi: 10.1021/acs.jpclett.5b01629

PAPER VII: H. Takala, S. Niebling, O. Berntsson, A. Björling, H. Lehtivuori, H. Häkkänen, M. Panman, E. Gustavsson, M. Hoernke, G. Newby, F. Zontone, M. Wulff, A. Menzel, J.A. Ihalainen, S. Westenhoff, "Light-induced structural changes in a monomeric bacteriophytochrome", *Structural Dynamics* **3**, 1-12 (2016), doi: 10.1063/1.4961911

PAPER VIII: P. Edlund, H. Takala, E. Claesson, L. Henry, R. Dods, H. Lehtivuori, M. Panman, K. Pande, T. White, T. Nakane, O. Berntsson, E. Gustavsson, P. Båth, V. Modi, S. Roy-Chowdhury, J. Zook, P. Berntsen, S. Pandey, I. Poudyal, J. Tenboer, C. Kupitz, A. Barty, P. Fromme, J.D. Koralek, T. Tanaka, J. Spence, M. Liang, M.S. Hunter, S. Boutet, E. Nango, K. Moffat, G. Groenhof, J.A. Ihalainen, E.A. Stojković, M. Schmidt, S. Westenhoff, "The room temperature crystal structure of a bacterial phytochrome determined by serial femtosecond crystallography", *Scientific Reports* **6**, 35279 (2016), doi: 10.1038/srep35279

Contribution report

PAPER I: I contributed to the structural analysis of the X-ray scattering data.

PAPER II: I purified a small fraction of the samples. I took part in the planning and execution the X-ray solution scattering experiments. I performed the structural analysis of the X-ray scattering data and contributed to the writing of the paper.

PAPER III: I designed the research together with my supervisor and our collaborators. I coordinated the work, planned, applied for beamtime, executed and analyzed the X-ray scattering experiments, analyzed the data and took major part in writing the paper.

PAPER IV: I designed the research together with my supervisor and our collaborators. I coordinated the work, planned, applied for beamtime, executed and analyzed the X-ray scattering experiments, analyzed the data and took major part in writing the paper.

PAPER V: I came up with the idea for this project together with our collaborators and together with my supervisor we designed the research. I coordinated the work, planned, applied for beamtime, executed and analyzed the X-ray scattering experiments, analyzed the data and wrote the manuscript.

Abbreviations

Here follows a list and short explanation of the different abbreviations used in this thesis.

APS	**A**dvanced **P**hoton **S**ource (synchrotron radiation facility outside Chicago)
BioCARS	**Bio C**enter for **A**dvanced **R**adiation **S**ources (beamline at the APS)
***Bs*YtvA**	*Bacillus subtilis* **YtvA** (photoreceptor protein)
CA	**C**atalytic **A**TP binding (protein domain, HK subdomain)
CBD	**C**hromophore **B**inding **D**omain (PAS and GAF domains together)
CCD	**C**harge **C**oupled **D**evice (type of detector)
cSAXS	**c**oherent **S**mall **A**ngle **X**-ray **S**cattering (beamline at the SLS)
CTT	**C**arboxy **T**erminal **T**ail (small part of *Dm*Cry)
DHp	**D**imerization and **H**isitidine **p**hosphotransfer (protein domain, HK subdomain)
***Dm*Cry**	***D**rosophila **m**elanogaster* **Cry**ptochrome (photoreceptor protein)
***Dr*BPhy**	***D**einococcus **r**adiodurans* **B**acterio **Phy**tochrome (photoreceptor protein)
EPR	**E**lectron **P**aramagnetic **R**esonance (experimental technique)
ESRF	**E**uropean **S**ynchrotron **R**aditation **F**acility (synchrotron radiation facility outside Grenoble)
FAD	**F**lavin **A**denine **D**inucleotide (chromophore)
FMN	**F**lavin **M**ono**N**ucleotide (chromophore)
GAF	c**G**MP-specific phosphodiesterase-**A**denylyl cyclase-**F**hlA (protein domain)
HK	**H**istidine **K**inase (family of proteins/protein domain)
ID09b	**I**nsertion **D**evice **09b** (beamline at the ESRF)
LOV	**L**ight-**O**xygen-**V**oltage (protein domain)

MD	**M**olecular **D**ynamics (computer simulations of protein motions)
PAS	**P**er-**A**rnt-**S**im (protein domain)
PHY	**PHY**tochrome specific domain (protein domain)
SAXS	**S**mall **A**ngle **X**-ray **S**cattering (solution scattering technique)
SHK	**S**ensor **H**istidine **K**inase (family of proteins)
SLS	**S**wiss **L**ight **S**ource (synchrotron radiation facility outside Zürich)
TRXSS	**T**ime-**R**esolved **X**-ray **S**olution **S**cattering (solution scattering technique)
WAXS	**W**ide **A**ngle **X**-ray **S**cattering (solution scattering technique)
XFEL	**X**-ray **F**ree **E**lectron **L**aser (intense X-ray source)

Contents

Chapter 1

Introduction

Proteins have been recognized as important biological molecules for hundreds of years. Their characterization started in the 1800's and during the second half of the 20th century the structural characterization of proteins has skyrocketed. It has become obvious that proteins are essential to all known forms of life. They are the molecular machines that keep our bodies going. They allow us to see, feel and taste. Increased understanding of proteins is therefore a necessity for the understanding of life.

1.1 Protein structural dynamics

It has been known for decades that the function of proteins is closely related to their three dimensional structure. The first protein structure determined was that of myoglobin, in 1958 [1]. Since then about 130,000 protein 3D structures have been solved.

The vast majority of these structures have been solved by X-ray crystallography. This technique requires the proteins to order themselves on a lattice of identical copies to form a crystal. But proteins are not rigid bodies and they constantly undergo conformational rearrangements, both at equilibrium and when perturbed [2]. The conformational dynamics of proteins are nowadays considered to be as important as their structure [3, 4]. The dynamic modes of proteins can for simplicity be divided into two categories; equilibrium fluctuations and functionally relevant motions [2]. The equilibrium fluctuations are the small conformational rearrangements that occur constantly. In conventional crystallography this is to some extent captured by the Debye-Waller factor which contains information about

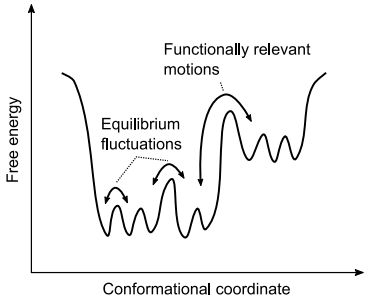

Figure 1.1: The free energy landscape of a folded protein. Equilibrium fluctuations are the constant movements between states of similar energy, typically on a pico- to nanosecond timescale. Functionally relevant motions occur on longer timescales, micro- to milliseconds, and require the crossing of extensive energy barriers.

how uncertain an atomic position is due to thermal fluctuations [5, 6]. Functionally relevant motions often require passing extensive energy barriers and they typically occur when the protein is perturbed, for example by binding a substrate or absorbing the energy of a photon (Figure 1.1).

The investigation of these motions is by no means a trivial task. Different spectroscopic methods can and have been applied, but they all come with their own limitations. Absorption spectroscopy gives information on electronic or vibrational transitions. This information is often crucial to understand how a protein works, but it is not directly linked to the structure of the protein. In some cases crystallography can be used to study the dynamics of proteins [7–16] thereby giving structural and dynamic information with high resolution. Any type of crystallography still requires the formation of crystals. Crystals, by their very nature, are likely to hinder larger scale conformational transitions and in many cases it is difficult to grow crystals of a suitable quality. Because of this, complementary techniques are required. Molecular dynamics (MD) simulations can be used to study equilibrium fluctuations with a high spatial resolution [17]. These methods, however, are still too inaccurate and computationally intensive to study conformational transitions on timescales longer than nano-, or at best microseconds.

At the intersection of X-ray crystallography and absorption spectroscopy

lies X-ray solution scattering, a solution based technique directly sensitive to the three dimensional structure of the protein. This technique, together with MD simulations, enables the direct study of conformational rearrangements of proteins, in solution, in real time.

1.2 Photoreceptor proteins

All organisms need to be able to sense and react to a wide range of environmental cues. One of the most important environmental signals is light, and many of the organisms on Earth need to adapt in response to light. This is achieved through dedicated proteins called photosensors or photoreceptors. These proteins regulate processes such as phototropism, shade avoidance, visual perception and the circadian rhythm.

Because the protein backbone or amino acid sidechains do not absorb visible light many photoreceptor proteins have chromophores embedded within the protein matrix. Since the chromophores are partly unsaturated the electrons can be delocalized across a conjugated π system by the energy of a visible photon. The larger the chromophore, and the conjugated π system, the easier the electrons are delocalized and longer wavelengths can be absorbed. Examples of chromophores are the blue light absorbing flavins and the red to far red light absorbing bilins.

The absorption of a photon by the chromophore triggers changes in the local environment of the chromophore; for example isomerization [18], bond formation [19], or electron transfer [20]. These changes have to be relayed through the protein as conformational rearrangements in order to enable interactions between the photoreceptor and downstream proteins and processes, thereby passing on the signal.

Many photoreceptors are constructed in a highly modular manner, where a few sensory domains can be coupled to a wider variety of effector domains. Some different photoreceptor families and their spectral sensitivity can be seen in Figure 1.2.

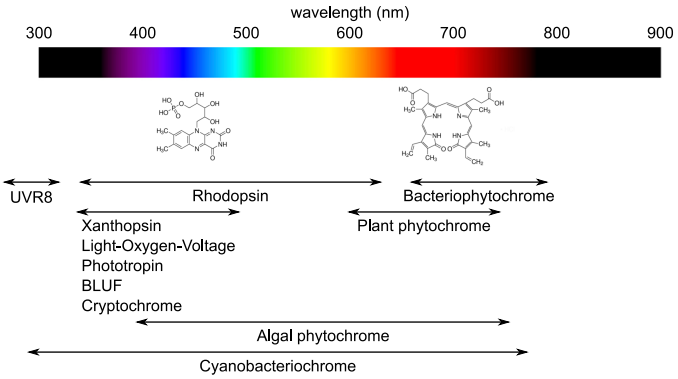

Figure 1.2: Spectral range of photoreceptors. Depending on the chromophore, photoreceptor proteins are sensitive to light ranging from the UV to near-IR wavelengths.

1.3 Sensor histidine kinases

To a large extent, bacteria rely on proteins called sensor histidine kinases (SHKs) to gather information about their surroundings. Together with other proteins, known as response regulators, SHKs make up so called two-component systems. Such arrangements are, apart from bacteria, also found in plants and certain other eukaryotes [21, 22].

SHKs can detect a wide range of signals, such as chemicals, pH changes, or light. These signals trigger structural changes and the activity of the histidine kinase output domain is modulated. The histidine kinase can be in a kinase active state where a conserved histidine residue within the kinase domain is phosphorylated prior to phosphotransfer to the response regulator. It can also be in a phosphatase state were a phosphate group is removed from the response regulator, thereby assisting in shutting down the signaling pathway [23].

Canonical SHKs are membrane spanning, homodimeric proteins. They consist of an extracellular sensor domain, a helical domain that traverses the cell membrane, commonly a PAS, GAF or HAMP domain and a coiled coil linker connecting it to the kinase domain. The kinase domain in turn comprises two subdomains; the dimerization and histidine phosphotransfer

(DHp) domain, which contains the phosphoaccepting histidine, and the catalytic and ATP-binding (CA) domain which have an ATP binding site. Since many SHKs are membrane spanning proteins, and because the interaction between the CA and DHp domain is rather loose it is difficult to study the entire protein. There are only a few solved structures comprising both sensor and effector domain, and these are from soluble members of the SHK family [24, 25].

As the overall topology has become understood focus has shifted towards characterizing the phosphoryl transfer [26, 27], the interaction with phosphoacceptor proteins [28], and how structural changes control the switching between phosphatase and kinase activity [29]. An important part in this deeper understanding of SHKs is to find out how external signals structurally modulate the activity of the histidine kinase domains.

The red light sensing phytochromes and the blue light sensing kinase YF1 investigated in this thesis are examples of SHKs.

1.4 Scope of this thesis

In this thesis time-resolved X-ray solution scattering has been used to interrogate the light-induced conformational changes in different photoreceptor proteins. I have grouped this work into the following chapters.

Chapter 2 will give a brief introduction to the basics of X-ray (solution) scattering.

Chapter 3 will describe how a time-resolved X-ray solution scattering experiment is conducted. It will also explain how the data can be analyzed in order to recover the structural information encoded within the scattering curve.

Chapters 4-6 will focus on the structural and dynamic information that time-resolved X-ray solution scattering has provided for a couple of different photoreceptor proteins, belonging to the phytochrome (**Papers I** and **II**), LOV domain containing (**Papers III** and **IV**) or cryptochrome (**Paper V**) protein families.

Finally, **Chapter 7** will summarize, conclude and provide an outlook.

Chapter 2

X-ray scattering

X-rays are electromagnetic radiation with a wavelength of ca. 1 Å. This is similar to the length of a chemical bond and the reason why X-ray scattering is a commonly used probe to study the molecular structure of anything from salts and minerals to proteins. In section 2.1 of this chapter I will detail the basic principles of X-ray scattering and how this changes when you study proteins suspended in a solution. In section 2.2 I will discuss how solution scattering patterns can be predicted from atomic coordinates.

2.1 X-ray scattering fundamentals

As an X-ray photon strikes an electron the electron begins to oscillate and emits radiation of the same wavelength as the incident X-ray. This phenomenon is called elastic scattering or Thomson scattering. Inelastic X-ray scattering (or Compton scattering) as well as absorption of the X-ray photon can also occur but this topic will not be covered in this thesis.

Scattering by a group of electrons. When calculating the scattering amplitude for any group of electrons, be it an atom or a molecule, the waves originating from each electron are summed, taking into account the shift in phase due to the separation between the electrons [30, 31]. The sum of the scattered waves for N electrons at $\mathbf{r_n}$ around an atom centered at O as shown in Figure 2.1A is given by equation 2.1. The incident and scattered wave vectors are represented by $\mathbf{k_i}$ and $\mathbf{k_s}$, respectively, and $|\mathbf{k_i}| = |\mathbf{k_s}| = \frac{2\pi}{\lambda}$, $\mathbf{q}=\mathbf{k_s}-\mathbf{k_i}$ is the momentum transfer with the modulus

q=$\frac{4\pi}{\lambda}sin(\theta)$, where λ is the X-ray wavelength and 2θ is the scattering angle and f_e is the scattering factor per electron.

$$F(\mathbf{q}) = \sum_{n=1}^{N} f_e e^{i\mathbf{q}\cdot\mathbf{r_n}} \tag{2.1}$$

For atoms where the electron density can be represented as spherically symmetric ($\rho(r)$) it is more convenient to calculate the so called atomic scattering factor, $f(q)$, according to equation 2.2.

$$f(q) = 4\pi \int \rho(r) r^2 \frac{sin(qr)}{qr} dr \tag{2.2}$$

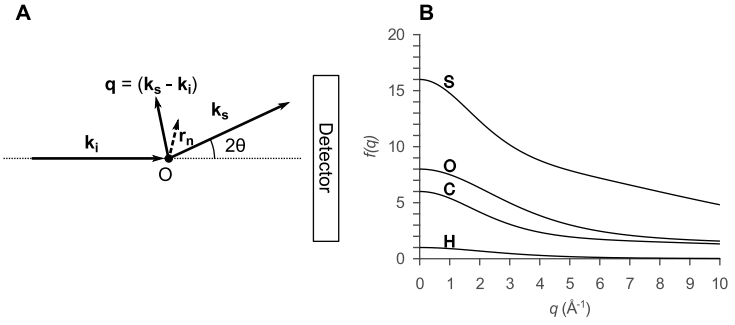

Figure 2.1: Scattering by an atom. (A) Incident radiation ($\mathbf{k_i}$) interacts with electrons indicated by $\mathbf{r_n}$ around an atom centered at O yield the scattered radiation ($\mathbf{k_s}$). The momentum transfer vector is **q** and the scattering angle is 2θ. (B) The atomic scattering factor, $f(q)$, for a few different elements.

At q=0 the factor $sin(qr)/qr$ approaches 1, so that the scattering amplitude is equal to the number of electrons. For other scattering directions the scattering amplitude is attenuated. This is because the distance between the electrons in an atom are about the same as the X-ray wavelength and partial destructive interference occurs. This effect is stronger at higher scattering angle (Figure 2.1B).

The scattering factor per electron in equation 2.1 can be exchanged for atomic scattering factor from equation 2.2 to calculate the scattering amplitude for a group of atoms located at $\mathbf{r_n}$. In a scattering experiment

one cannot directly measure the scattered wave, but rather it is the intensity that is recorded. The intensity is the product of the amplitude and its complex conjugate, $I(\mathbf{q})=F(\mathbf{q})F(\mathbf{q})^*$.

In solution all molecules are randomly oriented which spherically averages the phase factor. This leads to the Debye equation for the scattered intensity [30,32] (equation 2.3), where f_m and f_n are the atomic scattering factors and $r_{mn}=|\mathbf{r_m} - \mathbf{r_n}|$.

$$I(q) = \sum_m \sum_n f_m(q) f_n(q) \frac{sin(qr_{mn})}{qr_{mn}} \tag{2.3}$$

Bragg's law (equation 2.4) states that constructive interference will create intensity peaks for planes that are separated by a distance, r [33].

$$\lambda = 2rsin(\theta) \tag{2.4}$$

This is equivalent to defining the relationship between real space distances (r) and q according to equation 2.5.

$$r = \frac{2\pi}{q} \tag{2.5}$$

This equality is used to estimate the resolution in crystallography. It would be convenient if a similar relationship existed for solution scattering. As it turns out, each term in the Debye equation gives a positive contribution for $q<2\pi/r$, after which they decay whilst oscillating around 0 (Figure 2.2). Clearly, smaller distances will contribute more to the scattering at high angles whilst large distances only contribute to the scattering at the lowest angles. It is thus possible to say that the relationship between q and

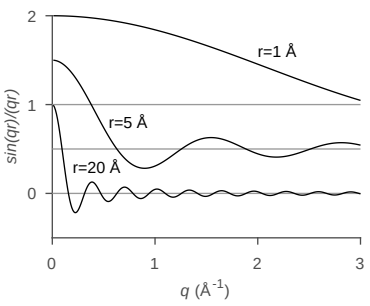

Figure 2.2: Debye terms. The q dependence of the Debye term for three different distances. The three curves are offset with respect to each other for clarity.

r given by equation 2.5 applies approximately to scattering from objects in solution.

In a real experiment the protein will be suspended in a buffer solution. This gives rise to yet another computational excursion. Apart from the scattered waves from the protein itself we must also consider the waves that would have been scattered by the bulk solvent, had the protein not been there, as well as the so called hydration layer, which is the solvent close to the solute that has a density different from that of the bulk solvent [34]. In total this surmounts to equation 2.6.

$$I(q) = \langle (F_{vac.} - F_{excl.} + F_{hyd.})(F_{vac.} - F_{excl.} + F_{hyd.})^* \rangle \qquad (2.6)$$

Where $F_{\text{vac.}}$ is the scattering of the solute in vacuum, $F_{\text{excl.}}$ is the scattering of the excluded bulk solution, $F_{\text{hyd.}}$ is the scattering of the hydration layer and $\langle \cdots \rangle$ represents the average over all orientations.

2.2 Predicting scattering from atomic coordinates

Predicting the X-ray solution scattering from atomic coordinates is by no means trivial and it is basically a field of research in its own. Several methods exist to predict scattering, all slightly different from each other (eg. [35–39]). The major difference between the different prediction schemes is how they compute the spherical average, how they deal with the excluded solvent, and how they represent the hydration layer [40]. In general, a trade-off has to be made between accuracy and computational efficiency.

Spherical averaging. There are three common methods for calculating the orientational average. The first one is the Debye equation (equation 2.3) [32]. This method involves a double summation and the computational cost scales with the number of atoms squared. An alternative way of performing the orientational averaging is to use spherical harmonics

where the Debye equation is expressed as a series containing Bessel functions and spherical harmonics [41]. Thanks to the orthogonality properties of spherical harmonics the double summation is reduced to a single sum and the computational cost scales linearly with the number of atoms. A third method which is mostly used with scattering calculations that involve molecular dynamics simulations is to numerically average over several different orientations (typically around 100) [39].

The excluded solvent. The most widely applied strategy to account for the excluded solvent when calculating X-ray scattering is by correcting for it by adding a term to the atomic scattering factor. From each scattering factor the scattering of a Gaussian sphere with electron density of the bulk solvent is subtracted (equation 2.7).

$$f_{corr.}(q) = f_{vac.}(q) - V\rho_{sol.}e^{-V^{2/3}\frac{q^2}{4\pi}} \tag{2.7}$$

Where $f_{\text{vac.}}$ is the scattering factor in vacuum, V is the volume of the scatterer and $\rho_{\text{sol.}}$ is the electron density of the bulk solvent. This strategy was initially proposed by Fraser [42] and is used by for example *CRYSOL* [35] and FoXS [38]. A problem with this strategy is that it introduces gaps and overlaps (Figure 2.3A) which affects the calculated scattering at higher angles.

An alternative approach, used in SASTBX [37] and SoftWAXS [36] defines the excluded solvent as the volume inside some surface. This is then divided into smaller volume elements before calculating the scattering from the excluded solvent (Figure 2.3B). In WAXSiS the contribution of the excluded solvent is calculated by subtracting the solute volume from a pure solvent MD simulation [39].

The hydration layer. It is well known that the solvent closest to the solute has properties that differ from that of the bulk solvent [34, 43–47]. Scattering studies show that the solvent arranges in several shells of higher density around the solute [44, 47] and this has to be dealt with when predicting the scattering curve of a protein from atomic coordinates.

A common strategy is to assume that the hydration layer has a homogeneous thickness and density different from that of the bulk (eg.

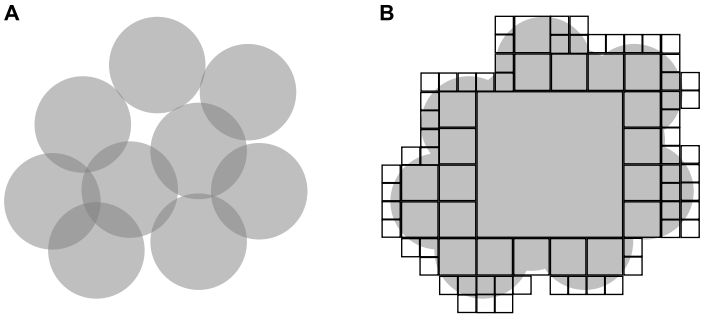

Figure 2.3: The excluded solvent. (A) Correcting the form factors with the sum of Gaussian spheres with the radius of the average atomic radius causes gaps and overlaps. (B) An alternative approach is dividing the volume enclosed by some surface into small volume elements.

CRYSOL or SASTBX). As has been shown, both by experiments and simulations [43, 46] this is a simplification and in reality the hydration layer has varying thickness and internal structure.

In *CRYSOL* the hydration layer is computed by using an angular function, $F(\omega)$, to define the surface [35] (Figure 2.4A). In short, the function is starting from the center of mass of the protein and working its way outwards in a defined direction (ω). When the distance from the current protein atom to the next atom is longer than some defined distance, this is the surface. This strategy works well for proteins that are "near" spherical and don't have a rough surface. SASTBX can deal with complicated surfaces much more efficiently thanks to the use of Zernike polynomials and a voxelization procedure similar to the cubic decomposition seen in Figure 2.3B [37]. The program FoXS accounts for the hydration layer in another way [38]. In FoXS the hydration layer is computed by adjusting the atomic scattering factor based on solvent accessibility. This strategy will cause an inhomogeneous hydration layer with overlapping density and gaps, and is therefore not a correct description either.

There exists software that explicitly simulates the protein in a solution, allowing the hydration layer to take whatever shape and density is energetically favorable. One such example is WAXSiS [39]. Arguably, such a treatment should produce the most correct results, however, at a very

high computational cost.

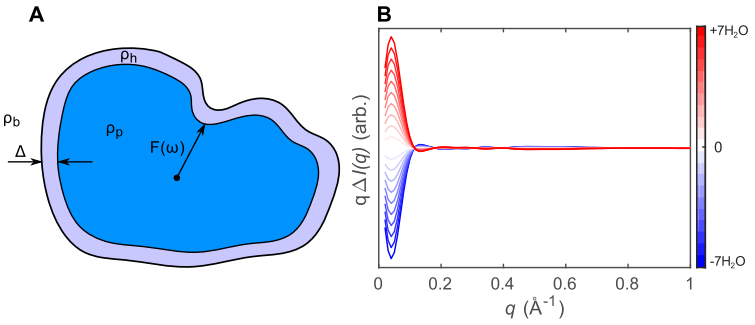

Figure 2.4: The hydration layer. (A) Representation of protein and hydration layer as they are treated by *CRYSOL*. The protein electron density is $\rho_{\mathbf{p}}$, the bulk solvent is $\rho_{\mathbf{b}}$, the uniform density of the hydration layer is $\rho_{\mathbf{h}}$, the hydration layer thickness is Δ and the angular function describing the envelope is $F(\omega)$. (B) Altering the contrast of the hydration layer around *Drosophila melanogaster* cryptochrome equivalent to the addition or removal of a few water molecules will have a significant effect on the scattering at low angles.

The effect that the hydration layer has on the total scattering is exerted by essentially changing the contrast between the solvent and solute(+hydration layer). Such effects are generally only expected for low angles [48]. To asses what effect this has the structure of the *Drosophila melanogaster* cryptochrome was chosen. The scattering was computed using *CRYSOL* and the density of the hydration layer was varied, whilst the structure was kept constant. The curve representing the default hydration layer density was then subtracted from the others, generating a series of difference scattering curves (Figure 2.4B). Based on this we can see that the hydration layer mainly affects the scattering curve at q<0.1 Å^{-1} .

How much do these simplifications matter? The work in this thesis is mainly focused on structural *change* and thus mainly deals with *difference* scattering curves. To test the impact that the simple models of excluded volume and hydration layer used by *CRYSOL* [35] have on difference scattering curves the results were compared to those obtained using

WAXSiS [39]. The difference scattering for *Deinococcus radiodurans* bacteriophytochrome (*Dr*BPhy) photosensory module was calculated. This protein undergoes a large conformational change and likely a large change of the hydration layer as well. In principle it is not possible to make a direct comparison because in *CRYSOL* all atoms are fixed, whilst in WAXSiS the sidechain atoms are allowed to move, something that can be expected to mostly influence the scattering at higher angles. Despite this and despite all the simplifications of *CRYSOL* with regards to the hydration layer as well as excluded solvent scattering it is clear from Figure 2.5 that the difference scattering is qualitatively similar for $0.05\text{Å}^{-1} \leq q \leq 0.6\text{Å}^{-1}$. Due to the spherical harmonics reconstruction along with the inhomogeneously filled excluded solvent *CRYSOL* is expected to start to break down at q=0.4Å^{-1} [35], but we can see that there is still reasonable agreement until q=0.6Å^{-1}.

It should be noted that since the *Dr*BPhy undergoes a huge conformational change this will overshadow much of the model inadequacy. For the cryptochromes investigated in **Paper V** the signal, and thus expected degree of conformational change, is much smaller. Moreover, the main features of this signal can be found $q < 0.2\text{Å}^{-1}$ and $q > 1\text{Å}^{-1}$, where the simpler models like *CRYSOL* perform poorly. In summary, if there is substantial difference scattering signal in the region $0.1\text{Å}^{-1} \leq q \leq 0.6\text{Å}^{-1}$ these can be modeled relatively well using for example *CRYSOL*, whereas features at higher or lower q require the use of a more comprehensive model.

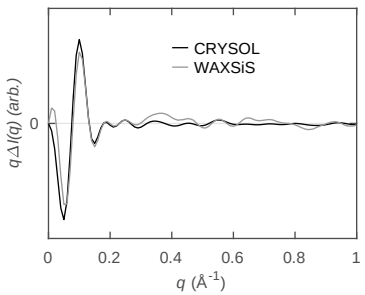

Figure 2.5: Comparison: *CRYSOL* vs WAXSiS. Predicted difference scattering for *Dr*BPhy photosensory module calculated by *CRYSOL* and WAXSiS.

Chapter 3

Time-resolved X-ray solution scattering

When using the term time-resolved X-ray solution scattering (TRXSS) I will be referring to a difference scattering technique. In the literature you will find terms such as time-resolved SAXS [49], time-resolved WAXS [50], time-resolved liquidography [51] etc. which, in these cases, are all the same technique. It is also possible to do conventional SAXS in a time-resolved manner, also referred to as time-resolved SAXS [52], but in this case the data treatment and analysis follows a different path and I will not go into further details regarding this technique.

About ten years ago TRXSS was applied to study light-induced conformational changes in proteins for the first time [53, 54]. Before this the method had mainly been used to study the conformational dynamics of small photoactive molecules [51, 55–60] but the method is becoming more and more used to study the light-induced structural dynamics in proteins. A range of different proteins have so far been studied, providing insights into reaction pathways and conformational rearrangement [49, 50, 53, 61–82].

This chapter is divided into three sections. In section 3.1, I will explain how a TRXSS experiment is conducted and different aspects that have to be considered. In section 3.2, I will explain how the raw data is treated prior to the analysis, which will be detailed in section 3.3.

3.1 Conducting the experiment

In order to perform TRXSS experiments with a pico- to millisecond time resolution a high X-ray flux is an absolute necessity. Cammarata et al. estimated that in order to detect a difference scattering signal in haemoglobin it was necessary to collect ca. 10^{12} scattered photons [53]. Specialized beamlines at third generation synchrotron light sources, such as BioCARS at the APS can deliver as many as 10^{10} photons in a pulse of ca. 100 ps duration [83] and only a fraction of those X-ray photons will scatter onto the detector. With the arrival of X-ray Free Electron Lasers (XFELs) with pulse lengths of ca. 10-100 fs and as many as 10^{12} photons per pulse it has become possible to investigate protein conformational changes on femto- to picosecond timescales (eg. [73, 75]). In this section different aspects of a TRXSS experiment will be described.

Triggering the reaction. The proteins under investigation in this thesis are photoreceptor proteins, meaning that they are designed to detect and respond to specific wavelengths. Accordingly, a conformational change can be triggered by a laser flash of appropriate wavelength.

When investigating timescales on the order of pico- to nanoseconds it is worth thinking about the time it takes for a protein to move around in the solvent. The rotational correlation time is described by Stoke's law. For proteins in water the rotational correlation time expressed in nanoseconds equates to approximately 0.6 times the molecular weight expressed in kDa, which is about 20-100 ns for the proteins under consideration here. The probability of exciting a molecule is proportional to $cos^2\alpha$ where α is the angle between the laser polarization and the chromophore dipole orientation. So a 5 ns laser pulse may only excite a fraction of the molecules. Furthermore, the photoactivation efficiency will also depend on the chromophore excited state lifetime i.e. will a 5 ns pulse be enough to excite the chromophore one or multiple times.

There are several aspects to consider when deciding with what laser energy to excite the protein. Enough energy has to be deposited in order to excite a significant portion of the protein molecules. On the other hand too high laser power will cause a larger thermal response in the solvent

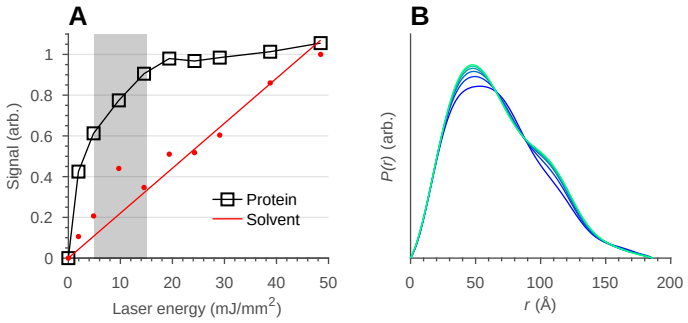

Figure 3.1: Photoconversion. (A) Photoconversion of *Dr*BPhy, measured for as the absolute difference signal in a certain *q*-range, as a function of the laser energy density. Solvent response as red dots with the linear fit as a red line. Shaded area marks the desired region, where the signal is high in comparison to the solvent heating. (B) *P(r)* calculated assuming different photoconversion efficiencies, going from low (blue) to high photoconversion (green).

(see paragraph on the thermal response of the solvent) and might potentially damage the protein. If possible, it is recommended to perform a laser energy titration as shown for the *Deinococcus radiodurans* bacteriophytochrome (*Dr*BPhy) in Figure 3.1A. This shows how the signal strength increases rapidly with increased laser energy, until a point when it plateaus. The ideal energy would be somewhere in the shaded region, where there is significant signal and before the signal levels off. Higher laser energies will almost exclusively add heat to the system.

Even if it is not possible to perform a thorough laser energy titration the photoconversion efficiency has to be correctly estimated. An over- or underestimation will effectively alter the resulting estimate of the pair distance distribution (*P(r)*) of the photoactivated conformation (Figure 3.1B) and thereby cause the refinement of the "wrong" structure. This is especially true if the data is modeled to one feature rather than several features over the entire *q*-range.

Detecting the scattering signal. Depending on the time range under investigation we used one of two different detection schemes; using either *photon counting rapid readout* detectors or *integrating charge coupled device (CCD)* detectors in a pump-probe setup. When investigating longer time delays (ms-s) rapid readout detectors are used [63]. In such an experiment the sample is exposed to a continuous train of X-ray pulses for several seconds whilst simultaneously reading out the detector. After a certain time the conformational change is triggered by a laser pulse. The result is two groups of detector images, *before* and different times *after* laser excitation. The time resolution in such an experiment is determined by the frequency of detector readout.

In our work at cSAXS we have used a Pilatus detector [84] that has been read out at 25 Hz, thereby achieving a time resolution of 40 ms with 35 ms X-ray exposure and 5 ms readout. This beamline is currently commissioning Eiger detectors [85], which can be read out approximately 1000 times as fast. However, this does not mean that the time resolution that can be achieved in practice will increase equally. As previously stated a fairly high number of scattered photons need to be recorded to resolve a difference scattering signal. This means that the acquisition cycle has to be repeated a vast number of times.

For shorter time delays ($\leqslant$ms) pump probe measurements using integrating CCD detectors are much more efficient. In this case a single or a short train of X-ray pulses are timed to arrive at a specific time after laser excitation and this is then repeated with a frequency of 5-20 Hz until enough photons have scattered onto the detector. Then the laser-X-ray time delay is changed and thereby a time-series of difference scattering curves is recorded. For comparison, one can think of the two detection schemes in terms of how a specific time delay will be revisited at least 5 times per second for the integrating CCD detectors, as compared to once in 5 seconds for the rapid readout detectors.

Thermal response of the solvent. Some of energy from the absorbed photon will dissipate into the solution, causing an increase in temperature and an indirect light-induced conformational change in the solvent. The scattering signature of the solute will thus be convoluted with that of the heated solvent (Figure 3.2).

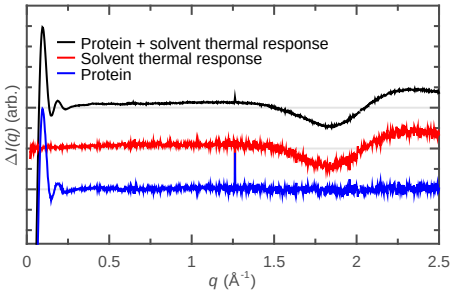

Figure 3.2: Solvent heating. When a photon is absorbed by the chromophore, some of the absorbed energy will dissipate to the solvent as heat. This causes a pronounced negative feature at $1.5<q<2$ Å^{-1} due to the change in water-water distances. By adding heat directly to the sample and solution with an infrared laser pulse the "pure heat" contribution can be isolated and subtracted from the data.

In order to deconvolute the data and obtain a "pure protein" signal it is necessary to record the "pure heat" signal and subtract this from the convoluted data. This is usually achieved by changing the excitation wavelength from the UV-vis range to the IR regime, thereby directly heating the solvent, but it can also be achieved by heating a dissolved dye [86].

Heating the protein-buffer solution with an IR pulse also provides a control measurement that proves that the difference scattering signal is due to light-induced, rather than heat-induced, conformational changes in the protein. Typically the temperature increase of the solvent observed in TRXSS experiments is on the order of 0.5-2 K and any significant protein related difference signal due to this amount of heat is yet to be observed.

Sample delivery and recovery. During the experiment the sample has to be kept in position at the X-ray/laser intersection. For this purpose we have used cylindrical quartz capillaries with an inner diameter of 1 mm and a wall thickness of 10 µm. The thin wall is important to keep the background scattering caused by the capillary as low as possible.

The sample has to be delivered to the correct position in the capillary. As this work was initiated the standard method for sample delivery was

to pump the sample back and forth through the use of a syringe pump. Mostly, this strategy works fine. At the turn of the pump, however, the scattering signal is drastically altered, presumably due to pressure changes. We initially dealt with this on the data reduction step, where the gross alterations to the scattering curve were recognized by the applied outlier rejection schemes. Later on, we stored the direction of the pump in a log file, and thus images recorded close to the turn of the pump could be preemptively disregarded. However, both of these approaches discard a lot of data. The solution turned out to be to exchange the syringe pump for a peristaltic pump, which did not give rise to any pump related artifacts in the difference scattering data. We did not investigate exactly why this is the case, but one explanation may be that when using the syringe pump there was always a column of air separating the sample from the buffer in the syringe. When we used a peristaltic pump the tubing was always filled with liquid, i.e. no compressible air columns.

To be able to perform the experiment with an efficient duty cycle, and without having to prepare extreme quantities of sample, the protein has to somehow be reverted from its light adapted state back to the dark state. The phytochrome proteins studied at first are in many ways a biophysicist's dream; they are very stable proteins, have a very stable light adapted state, and their resting state can easily be recovered by a laser flash. As the focus was shifted to studying light-oxygen-voltage (LOV) proteins complications arose. In LOV photosensors the resting state cannot be easily recovered through a laser flash of appropriate wavelength. At 20 °C the photoproduct state of the LOV domain from *Bacillus subtilis* YtvA is stable for 1000's of seconds. This is strongly dependent on temperature and so the setup was designed to keep the protein in a reservoir at 35 °C when not in the X-ray/laser intersection. The cryptochrome samples posed yet another possible problem; the dark adapted state could not be recovered by a laser flash, neither was its recovery particularly temperature sensitive. In this case the dark adapted state can be sufficiently recovered by adding an oxidizing agent in the form of potassium ferricyanide to the buffer. This promptly recovers the dark state of the chromophore within seconds and ensures that the experiment can proceed with a reasonable duty cycle.

Concentration effects.
The scattering signal scales linearly with concentration but high protein concentration also comes with side effects. At low scattering angles (q<0.1Å^{-1}) interparticle interference caused by high protein concentration may cause a depression of the scattering curve. By collecting data at several different concentrations this can be dealt with by a) finding out which is the affected region and disregarding this in the analysis (**Paper III** and **IV**) or b) finding out the quantitative effect and accounting for it. This is done by either diluting the sample until the (difference) scattering curve no longer changes shape (**Paper II**, see Figure 3.3) or by diluting it a few times and thereafter extrapolating to infinite dilution [77]. Then the data from the diluted sample are merged with data from the concentrated sample in some region where concentration does not affect the shape of the scattering curve. An alternative approach is to scale the data by the packing structure factor as in ref. [77].

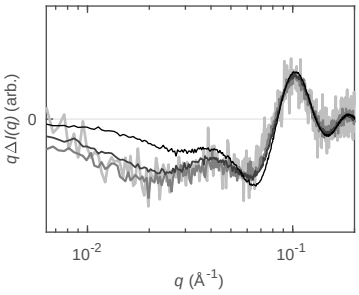

Figure 3.3: Concentration effects. Interparticle interference affects the scattering at low angles. Diluting from high (black and thin) to low (light gray and fat) concentration removes these artifacts.

Radiation damage. As the protein is exposed to intense X-ray radiation some of the X-ray photons will elastically scatter and some will deposit at least parts of their energy in the protein [87]. This will cause the breakage of bonds and formation of reactive species that will alter the protein structure. The flavin chromophores present in some of the proteins investigated in this thesis are particularly sensitive to reduction by X-rays. A combined crystallography and Raman spectroscopy study showed that a radiation dose of about 9 MGy can cause photoreduction of the flavin chromophore under cryogenic conditions [88].

The TRXSS experiments herein are conducted at ambient temperature and are therefore even more sensitive, doses as low as 10 kGy may cause radiation damage [89]. Using the software *RADDOSE* [89], the radiation doses for the TRXSS experiments presented in this thesis are estimated to

be <10 kGy before the exposed sample is replaced by fresh sample. In addition many of the buffer solutions used contain large amounts of glycerol, which helps protect against radiation damage. We have noted though, that glycerol concentrations $\geqslant$20% v/v actually appears to promote radiation damage, even in buffer without any protein present. Presumably this is radiolysis of water because at such high glycerol concentrations the sample becomes too viscous and is not replenished between X-ray exposures.

Since TRXSS cannot provide atomistic information itself we do not have to worry too much about the small structural alterations caused by moderate radiation damage (Figure 3.4A). To ensure that radiation damage that renders the protein completely inactive does not affect the data the experiment is usually designed so that *laser off* images are interleaved with the *laser on* images. When using rapid readout detectors this means collecting every other dataset without laser excitation and then subtracting the *laser off* dataset from the *laser on* dataset. This ensures that drifts, such as the protein degradation caused by radiation damage, is effectively subtracted when calculating the difference scattering (Figure 3.4B).

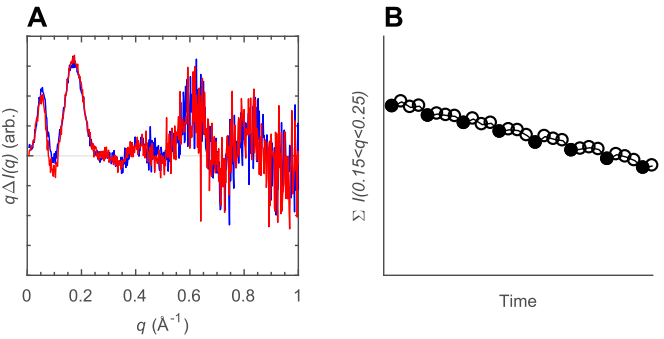

Figure 3.4: Radiation damage. (A) Difference scattering of the YtvA LOV domain recorded at two different times, separated by ca. 500 s of intense X-ray exposure. (B) Dark images are interleaved (solid black circles) which makes it possible to subtract radiation damage (and other experimental drifts).

3.2 Processing the data

Following the TRXSS experiment the data has to be processed before more detailed analysis is performed.

Radial integration and image corrections The scattering data is initially recorded on a 2D area detector, but all the scattering data presented in this thesis are 1D curves. The process by which the 2D detector image is transformed into a 1D curve is called radial integration, or azimuthal averaging. Since the sample has a random orientation, the scattering pattern should be isotropic and the scattering should be the same at a defined radius, regardless of the azimuthal angle.

Because synchrotron radiation is polarized, the scattering pattern will actually not be completely isotropic. The detector will likely have a few pixels with a different responsiveness compared to most pixels. Such pixels, along with pixels close to the beamstop, are usually masked. If the detector used is a CCD detector it cannot directly detect the scattered X-ray photon, but a phosphorescent screen is used as a relay between the X-ray photon and the detector. Accounting for the polarization of the X-ray beam, mask, phosphorescence, as well as a few other corrections are performed in connection with the radial integration. This is usually done using software controlled by staff at the beamline, since they know exactly what applies to their X-ray source and detector [90]. I will therefore not go into further details regarding this.

Monochromatic and polychromatic X-ray radiation Different beamlines are geared towards different tasks. Beamlines with a focus on recording data with a high temporal resolution will typically not have a monochromator, since the insertion of one reduces the photon flux by roughly a factor 10. As an effect the X-ray beam at such beamlines will contain a distribution of a number of different wavelengths (Figure 3.5). This will cause smearing of the data and is something that should be considered when comparing data recorded with a monochromatic or a polychromatic beam, or when comparing predicted scattering with recorded

scattering [53]. Fortunately, a monochromatic scattering curve can relatively easily be transformed to a polychromatic scattering curve, if the wavelength distribution of the polychromatic X-ray beam is known [91].

Difference scattering curves

During the experiment the X-ray scattering of a protein solution with dark adapted or illuminated sample are recorded, and the curves subtracted from each other. In general both the dark adapted and illuminated protein have very similar overall structure and thus the difference in scattering is small. It is common procedure to normalize the scattering data at $q \approx 1.5 Å^{-1}$ or $q \approx 2.1 Å^{-1}$ because in these regions the water scattering has an isosbestic point with respect to heating [53,64]. Typical signal strengths on this normalized scale are on the order of 1% (see Figure 3.6).

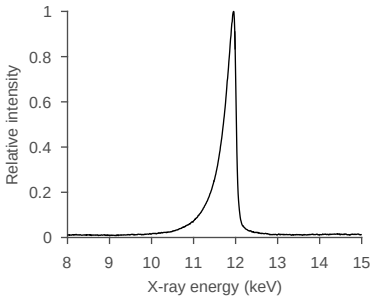

Figure 3.5: Polychromatic radiation. Energy distribution for the polychromatic X-ray beam at BioCARS at the APS.

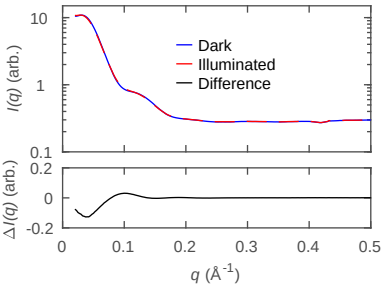

Figure 3.6: Difference scattering. The two X-ray scattering curves representing dark and illuminated phytochromes are almost impossible to distinguish, yet there is a definite and reproducible difference scattering signal.

In a conventional SAXS experiment such differences are generally below the detection limit. At least two measurements are performed in a conventional SAXS experiment: i) the protein and buffer, ii) only the buffer. These contributions have to be correctly scaled so that the scattering can be calculated as: $I_{\text{Protein}} = I_{\text{Protein+Buffer}} - I_{\text{Buffer}}$. This is repeated both for the dark sample and the light sample, thereby giving rise to a wealth of experimental errors. The way that a TRXSS experiment is designed enables the direct

subtraction of the dark scattering curve from the light one, without separately recording the buffer scattering and correctly scaling this. As shown in Figure 3.4 even radiation damage and other drifts effectively cancel out when calculating a difference scattering curve.

Removing outliers As is the case for almost all real experiments, for one reason or the other, some of the data will be corrupted. It is essential to have a robust strategy for dealing with such outliers. The strategy we chose is to observe the scattering at $q>1.5$ Å^{-1} where the contribution of the protein signal is very small and the contribution of the well characterized water scattering is the highest. Curves differing from the median scattering in this region by more than a few percent or a couple of standard deviations can be considered outliers and are removed.

Removing the solvent thermal response Before any structural analysis of the scattering curves is performed the solvent thermal response has to be treated. The scattering fingerprint of solvent heating is recorded as previously described. This is then scaled to the regular experiment difference signal in a region where water scattering dominates ($q>1.5$ Å^{-1}) and subtracted.

3.3 Analyzing and interpreting the data

In this section I will outline several of the possible strategies that can be applied to TRXSS data analysis and discuss the strengths and weaknesses of respective analysis method.

Kinetic analysis and spectral decomposition. Following a successful TRXSS experiment one of the first treatments of the data will usually be to reduce the complexity of the set of difference scattering curves. At this point TRXSS is no different than any other spectroscopic technique and it is common to view each TRXSS difference scattering curve as a linear combination of a set of basis spectra, representing the difference scattering of particular intermediate conformations. The basis spectra can be obtained in different ways: by singular value decomposition, principal

component analysis or kinetic analysis in which a certain kinetic model is imposed on the data. Frequently the decomposition of the TRXSS data involves a combination of these methods.

Information content. When performing structural analysis of difference scattering curves it is important to remember that the information content in a X-ray solution scattering curve is fairly low. The number of independent data points (n_s) can, based on work by Shannon [92], be estimated by

$$n_s = (q_{max} - q_{min}) \cdot \frac{r_{max}}{\pi} \tag{3.1}$$

where q_{min}/q_{max} are the lowest and highest angles to which reliable data have been collected and r_{max} is the maximum dimension of the protein [93,94]. A typical X-ray scattering curve thus has about 10-50 independent data points. This is considered to be the *minimum* number of parameters that can be determined from the information in the scattering curve [93].

If it is possible to record anisotropic difference scattering data the amount of information can be doubled [49, 65]. This, however, requires that the TRXSS data is recorded before the protein reorients in the solution, which typically happens within tens of nanoseconds. In principle it is also possible to retrieve more information by observing so called spatial or angular correlations, as proposed by Kam in the 1970's [95]. This method, however, requires that the sample is frozen, either in space or in time as well as a very large number of scattered photons, for statistical reasons. Thus, this has today only been applied to very large structures such as viruses [96] or synthetic structures [97], or very dense elements such as gold [98] and primarily at XFELs. Clearly, in order to reach more detailed insights into photoreceptor signaling, the X-ray scattering has to be augmented with additional information.

Model free analysis. Evaluating what conformational changes that occur directly from the $\Delta I(q)$ curve is rather difficult. The information is located in reciprocal space which is difficult for us to visualize. Fortunately, this information can be transformed into real space, making it much easier to comprehend (Figure 3.7). The scattering curve ($I(q)$) is the Fourier sine

transform of the pair distance distribution function (*P(r)*), and by extension the *difference* scattering curve ($\Delta I(q)$) is the Fourier sine transform of the *change* in the pair distance distribution function ($\Delta P(r)$) as shown by equations 3.2a-b. The pair distance distribution function specifically contains information about the pairwise distance between the electrons in the sample.

$$\Delta P(r) = \frac{r}{2\pi^2} \int_{q_{min}}^{q_{max}} q\Delta I(q) sin(qr) \cdot e^{q^{-2}\alpha^2} dq \tag{3.2a}$$

$$\Delta I(q) = \frac{4\pi}{q} \int_{0}^{r_{max}} \frac{\Delta P(r)}{r} sin(qr) dr \tag{3.2b}$$

Since the *q*-range over which the scattering is collected is finite ($q_{min} \leqslant q \leqslant q_{max}$) the regularization/dampening function $e^{-q^2\alpha^2}$ is applied and a value of α chosen that generates a smooth $\Delta P(r)$ [30]. The only parameter that has to be known *a priori* is an approximate estimation of the maximum dimension of the protein (r_{max}). The larger the protein (larger r_{max}) the smaller q_{min} has to be so that the condition $q_{min} \leqslant \pi / r_{max}$ is fulfilled [93]. Structural evaluation of the difference scattering curve through this method has usually been more common for significantly smaller molecules [99] but it can still provide useful and model free information about structural changes in proteins (eg. **Paper III** and **Paper V**).

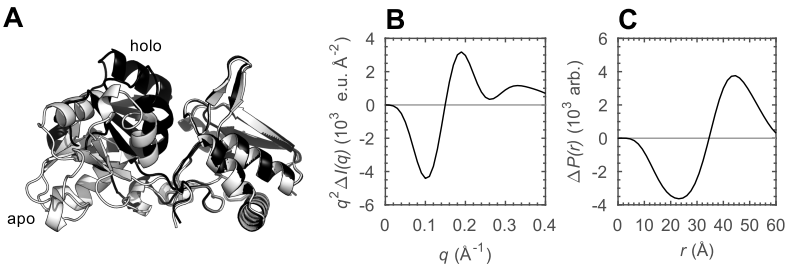

Figure 3.7: $\Delta P(r)$ transformation. (A) The structure of lysine- arginine-ornithine-binding protein (LAO) in apo and holo conformation (pdb id: 2LAO and 1LST). (B) Predicted difference scattering curves for LAO (I_{apo}-I_{holo}). (C) Transformation from $\Delta I(q)$ to $\Delta P(r)$ reveals what can be seen from the structures in (A), more long and less short distances in the apo conformation.

A structural parameter that can be assessed directly from the scattering curve is the radius of gyration (R_g). The R_g is the root mean square distance the the parts of the protein from its center of mass. This parameter will change if the general shape of the protein changes, but also if the shape of the protein remains the same but there is redistribution of mass within the protein [75]. The Guinier approximation is usually used to calculate R_g from absolute SAXS curves. This strategy can also be applied to difference scattering curves, according to equations 3.3a-b. The Guinier approximation describes the scattering at low angles as a Gaussian function. In general this approximation is considered valid for $q \leqslant 1.3/R_g$.

$$I(q) = I(q=0)e^{-q^2R_g^2} \tag{3.3a}$$

$$\Delta I(q) = I(q=0)(e^{-q^2R_{g,B}^2} - e^{-q^2R_{g,A}^2}) \tag{3.3b}$$

The Guinier approximation requires knowledge of the scattering intensity at zero angle (*I(q=0)*). This is one of the standard parameters estimated in a conventional SAXS experiment (as done in **Paper II**). It is also possible to obtain an estimate of *I(q=0)* because it is proportional to the the excess number of electrons in the scattering body compared to the surrounding buffer squared (section 2.1). This strategy was chosen by Levantino et al. in their study of protein quakes in myoglobin on femto- to picosecond timescales following photo dissociation of the carbon monoxide. The authors were able to observe oscillating values of R_g and the protein volume following laser excitation [75]. If a measurement or an estimation of the scattering, and thereby *P(r)* is available for one of the states, it is also possible to calculate R_g from *P(r)* through equation 3.4, instead of using the Guinier approximation.

$$R_g = \sqrt{\frac{\int_0^{r_{max}} r^2 P(r) dr}{2\int_0^{r_{max}} P(r) dr}} \tag{3.4}$$

The scattering at low angles is strongly dependent on the mass of the protein. This enabled Cho et al. to investigate the volume changes and mass transport in myoglobin on pico- to millisecond timescales as carbon monoxide dissociates, following photoexcitation [62].

***Ab initio* modeling.** More detailed structural insights can be obtained by *ab intio* modeling against scattering data. As stated previously; the information contained within a scattering curve is rather limited. Still, there is enough information to reconstruct the overall shape of proteins. Currently *ab initio* modeling is exclusive for absolute scattering curves which then has to be measured directly or recovered from a TRXSS difference curve as in ref. [77] or **Paper II**. After retrieving absolute scattering curves conventional SAXS analysis pipelines are used. First the *P(r)* is retrieved using GNOM [100]. After this the *ab initio* modeling is done by for example DAMMIN [101] or by GASBOR [31].

The limited information in the scattering pattern is not quite enough to uniquely reconstruct even overall shapes and additional information greatly enhances the reconstruction. One example is the dimeric nature of phytochromes as described in **Paper II**. To assess the convergence of the *ab intio* models it is recommended to perform several rounds of modeling and compare the outcome using for example DAMAVER [102]. Despite the coarse nature of the *ab initio* approach such models can reveal protruding domains [77] or reorientation of domains [82].

Rigid body modeling. The availability of high resolution structure(s) of resting, intermediate or active states of the protein opens up additional possibilities to obtain detailed structural information. An early adopted strategy for modeling TRXSS data was that of rigid body modeling. In the first ever application of TRXSS to study conformational changes in membrane proteins Andersson et al. recorded scattering data on bacteriorhodopsin and proteorhodopsin [50]. Based on available crystal structures they defined rigid bodies whose relative orientation and position were refined through iteratively reorienting the rigid bodies on a grid. Similar strategies have been used several times since [66, 67, 78, 103].

This modeling approach has two major drawbacks. The main one is probably the restricted conformational sampling space. The other is that it is difficult to judge whether the models are physically sensible if no measures are taken to ensure this. One way to alleviate this is to add a regularization step to the refinement algorithm as described by Malmerberg et al. [76]. The regularization step meant adjusting bond lengths, angles and dihedral angles to acceptable values.

Molecular dynamics. During the last years, analysis of TRXSS data has come to involve molecular dynamics (MD) simulations. Since MD was initially developed in the 1970's the typical simulation time has extended from a few picoseconds back then [17], to hundreds of nanoseconds or several microseconds (or even milliseconds) today [104, 105]. In the MD simulations under consideration in this thesis Newton's equations of motion are solved, numerically and stepwise [106]. This means that the simulations are *classical* (i.e. there are no quantum mechanical calculations). The forces are calculated from the potential energy, which in turn is governed by the atomic coordinates and the forcefield chosen. The forcefield provides restraints in the form of bond angles, bond lengths, dihedral angles etc. and thus ensures that the protein conformation is physically sensible. Coupled with TRXSS, MD simulations can provide meaningful insights into light-induced conformational transitions.

X-ray scattering guided molecular dynamics. In guided MD the scattering data is used to alter the energy landscape imposed by the MD forcefield. Done correctly this will bias the simulation towards structures in agreement with the scattering data, whilst still obeying the physical restraints of the forcefield, thereby generating physically meaningful structures. This strategy is by no means unique to TRXSS but is also used in for example NMR refinement [107]. To analyze TRXSS data by using it as a guide for MD simulations was an early idea. Already 2009 Ahn et al. [61] analyzed a difference scattering curve of myoglobin recorded at 10 ns after carbon monoxide photolysis using a rigid-body guided MD approach. The feasibility of this method was further demonstrated as the X-ray scattering guided MD tool was implemented in the MD software GROMACS [108].

This analysis scheme has the unfortunate drawback that it is computationally intensive and in the current implementation not easily parallelized. In addition, the choice of weighting parameters (how the MD forcefield is weighted with respect to scattering data) is still a complex task itself. In general it appears that guiding MD simulations work well when large parts of the protein undergo a concerted change, even if this change is small [109]. If this method is allowed to mature it could definitely become a major strategy for analyzing TRXSS data.

X-ray scattering filtered molecular dynamics. An alternative approach to X-ray scattering guided MD could be termed X-ray scattering *filtered* MD and this is the approach we took in **Papers I** and **III-V**. Rather than biasing the MD forcefield with information from scattering data, unperturbed equilibrium simulations are performed. The scattering from the different structures in the MD trajectory is then calculated, difference scattering curves are generated and compared to the experimental data and pairs of structures reproducing the difference scattering data are analyzed further. Essentially, the TRXSS data supply restraints to obtain the functionally relevant transitions from the sea of equilibrium fluctuations provided by the MD simulation. If atomistic models of potential intermediates are available from for example crystallography these can preferentially be used as initial structures for the simulations (eg. **Paper I** or [81]). However, in many cases there are no atomistic models available for these intermediate structures. Frequently the structures are only transiently formed and this is also part of the reason why TRXSS is an attractive technique; it provides structural information that is otherwise hard to come by. If this is the case then the MD simulation typically has to be biased in order to sample functionally relevant motions in addition to the equilibrium fluctuations around a relaxed structure. In their study of ultrafast conformational changes in photosynthetic reaction center Arnlund et al. generated biased simulations by depositing the energy of the absorbed photon as kinetic energy in the bacteriochlorophyll cofactors [73]. In our studies of light-oxygen or voltage (LOV) proteins (**Papers III-IV**) and cryptochrome photosensors (**Paper V**) we have used dark and light state parameters for the chromophore and active site to generate relaxed and excited simulations.

3.4 Summary

Time-resolved X-ray solution scattering provides direct information on structural transitions on timescales from femtoseconds to seconds. The resulting difference scattering curves can be analyzed to reveal the nature of the conformational change on a global, or if coupled with MD simulations, a more detailed level.

Chapter 4

Phytochromes

In **Paper I** and **II** we study the red light sensing proteins known as phytochromes. These proteins give bacteria, plants and fungi the ability to sense light, and absence thereof [110]. Phytochromes exist in two metastable states termed P_r and P_{fr}, which absorb red and far-red light, respectively [111, 112]. It is possible to reversibly switch between the two using red (P_r to P_{fr}) or far-red (P_{fr} to P_r) light. This is used to guide the organism from the shade (high far-red:red ratio) to the light (low far-red:red ratio). Typically, phytochromes have P_r as their resting state, these are referred to as canonical phytochromes, but some bacterial variants relax to P_{fr} in the dark and are called non canonical or bathy [113].

4.1 Phytochrome structure.

Most phytochromes are dimeric proteins and they exhibit a modular domain architecture. Following the discovery of bacterial homologs to plant phytochromes a range of three dimensional structures of the different domains were determined [71, 114–121]. The photosensory core consisting of a Per-Arnt-Sim (PAS), a cGMP phosphodiesterase-adenyl cyclase-FhlA (GAF), and a phytochrome specific (PHY) domain (Figure 4.1A) is conserved between phytochromes found in plants, bacteria and fungi. The PAS, GAF and PHY domains also share a similar structural core consisting of a five stranded β-sheet.

A bilin chromophore, responsible for the absorption of light, resides within the PAS or GAF domain, and is additionally in contact with the

PHY domain. The PAS and GAF domains assume a tightly packed, globular structure, which is stabilized by a knot formed by the backbone [114]. The PHY domain is connected to the GAF domain through a long helical spine and through the so-called PHY *arm* or *tongue*, which reaches back and contacts the chromophore on the outside of the dimeric protein [115, 116]. The PHY tongue is folded as a β-sheet in P_r and as an α-helix in P_{fr} [71, 115, 116].

On the C-terminal end of the phytochrome photosensor different output modules can be attached [122]. Cyanobacterial and bacterial phytochromes are usually sensor histidine kinases and the protein is the first part of a two-component signaling mechanism [110, 123]. The histidine kinase module comprises a dimerization and histidine-containing phosphotransfer (DHp) domain and a catalytic ATP-binding (CA) domain. The C-terminal domains of plant phytochromes resemble histidine kinases, but they lack the crucial histidine for phosphorylation. Instead, they function as serine/threonine kinases *in vitro* [124], which is just one of several biochemical output mechanisms *in vivo* [125–127]. There are no available three-dimensional crystal structures of complete phytochromes with their kinase output domains.

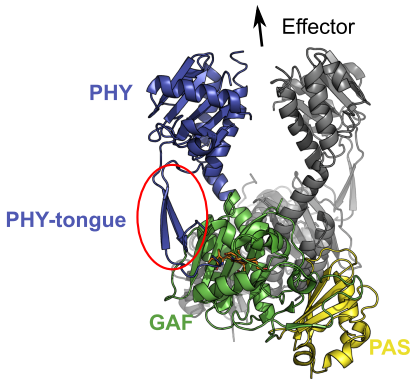

Figure 4.1: Phytochrome structure. Overall structure of phytochrome photosensory module.

4.2 Phytochrome photochemistry.

Using optical spectroscopy the photoconversion of phytochromes has been studied since the discovery of the protein in the 1950's. Phytochromes from different bacteria, cyanobacteria and plants have been investigated revealing several different intermediates [111, 128–135]. It generally appears that bacterial phytochromes exhibit the fewest spectral intermediates, cyanobacterial phytochromes are more complex, and plant phytochromes are the most complex.

The photoactivation of a bacterial phytochrome can be described by three intermediates, usually termed lumi-R, meta-Ra and meta-Rc (Figure 4.2) [128]. The first intermediate, Lumi-R, forms on a femto- to picosecond timescale [18] and converts into meta-Ra within microseconds [128]. Then a proton is released to the solvent to form the meta-Rc state within a few milliseconds and finally the photoproduct, P_{fr}, is formed in tens of milliseconds. In the last step partial proton uptake occurs [128, 131]. Structurally, the tetrapyrrole chromophore is thought to isomerize within picoseconds of excitation with red light [18]. Probably this step involves the *Z*-to-*E* isomerization of the C_{15}=C_{16} double bond, which leads to a rotation of the chromophore D-ring [11, 135, 136].

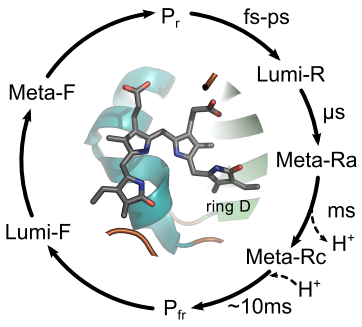

Figure 4.2: Phytochrome photocycle. The canonical photocycle of a bilin chromophore within a bacteriophytochrome PAS-GAF domain. In the center, a biliverdin in its binding pocket.

4.3 Signal transduction through a bacterial phytochrome

The photochemistry and local conformational rearrangements in the immediate proximity of the chromophore have been studied in great detail over the last decades. How these changes are relayed to the rest of the protein is much less investigated. Whereas some of my collegues have undertaken the challenging task of elucidating the atomistic rearrangements within the photosensory domain at the very early timescales (<ns) following light absorption using serial femtosecond crystallography (SFX) [137], my focus has been on investigating the global conformational rearrangements that follow using TRXSS. This work has resulted in **Paper I** and **Paper II**.

In **Paper II** we investigated how the signal was relayed through the phytochrome from the bacterium *Deinococcus radiodurans* (*Dr*BPhy). The protein was genetically separated into three fragments comprising the i) PAS-GAF domains, ii) PAS-GAF-PHY domains or iii) the complete protein. TRXSS experiments revealed conformational changes appearing for all three constructs on a millisecond timescale (Figure 4.3).

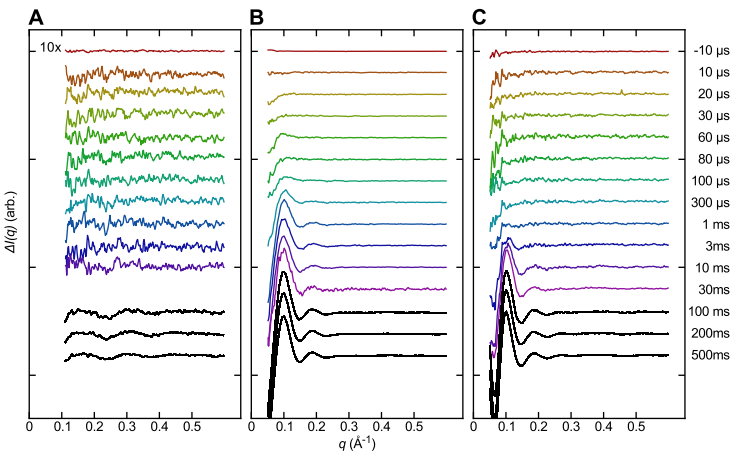

Figure 4.3: TRXSS data for *Dr*BPhy. (A) PAS-GAF, (B) PAS-GAF-PHY and (C) full length protein. Adapted from **Paper II**.

In conjunction with the TRXSS measurements, we also performed a series of transient absorption measurements in order to monitor the chromophore state. Overlaying the TRXSS kinetics with the absorption measurements puts the conformational transition between the Meta-Ra and Meta-Rc states of the chromophore (Figure 4.4). The structural rearrangements between Lumi-R and Meta-Ra are arguably very small, perhaps on the order of individual sidechain rearrangements given the low detection limit of TRXSS (eg. [62]).

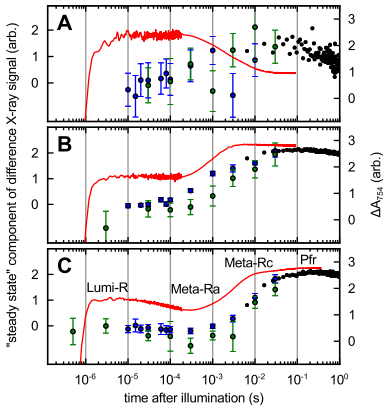

Figure 4.4: Photoconversion kinetics for *Dr*BPhy. (A) PAS-GAF, (B) PAS-GAF-PHY and (C) full length protein. Red lines show the absorbance at 754 nm and the blue, green and black markers represent data collected at ID09b, BioCARS and cSAXS respectively. Adapted from **Paper II**.

These data also revealed that the timescale of the structural photoactivation is similar for the three constructs (ca. 1, 2 and 6 ms half-rise time). This is a clear indication that it is the structural rearrangements within the PAS-GAF domain that are the rate limiting steps and that rearrangements involving the PHY and HK domains are only slightly affecting this. The Meta-Ra to Meta-Rc transition has previously been associated with a proton transfer to the surrounding solvent [128, 131] and it is possible that this event ultimately controls the structural activation of phytochromes.

4.4 Structural activation of the photosensory module

To pin down the structural events of phytochrome photoactivation we also conducted a combined crystallography and solution scattering study (**Paper I**) on the photosensory module of *Dr*BPhy, the PAS-GAF-PHY fragment. The three dimensional structures of dark and light adapted *Dr*BPhy were determined by X-ray crystallography and revealed two intriguing details (Figure 4.5). The first one is the PHY-tongue, which appears as a β-sheet in the dark adapted structure but becomes an α-helix under illumination. This was the first time these configurations were observed in the same phytochrome as they had previously only been observed separately [11, 115, 116, 118]. Since then this has been confirmed with spectroscopy [138–140] and through crystallography [121]. The second major feature is the increased separation of the PHY domains. In response to light the PHY-PHY distance increase by more than a nanometer.

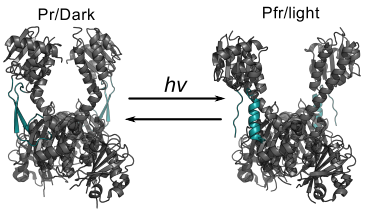

Figure 4.5: Crystal structures of *Dr*BPhy. Three dimensional structures of the photosensory module *Dr*BPhy in dark and light adapted states as determined by X-ray crystallography (pdb id: 4O01 and 4O0P). The tongue region (marked in teal) switches between β-sheet and α-helix and the PHY domains are separated.

We verified the crystal structures against TRXSS data through the use of filtered MD simulations starting from either the dark or light adapted crystal structure (see section 3.3). The scattering was calculated and compared to the experimental data in a pairwise manner (Figure 4.6A). This analysis revealed that the crystal structures actually do not fit the scattering data particularly well. They do however, capture the essence of the structural change. The difference between the crystal and solution structures lies in the more pronounced separation of the PHY domains in the light adapted state in solution compared to crystal as well as in the more "relaxed" or extended dark adapted state (Figure 4.6B). Presumably, this discrepancy is a result of the packing in the crystal.

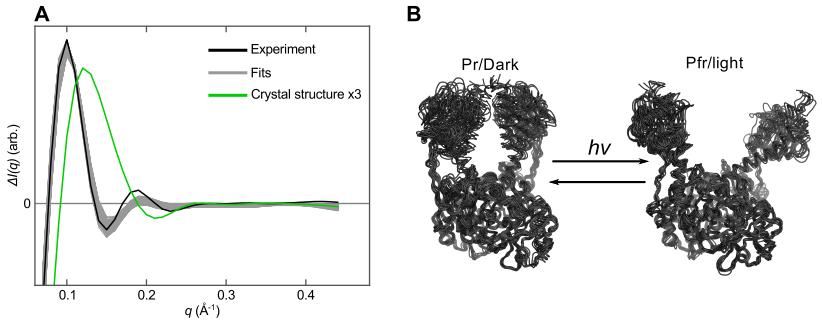

Figure 4.6: Refinement of crystal structures against TRXSS data. (A) The fit between calculated and experimental data for the 100 best pairs, compared to the fit of the crystal structures. Adapted from **Paper I**. (B) Structural ensembles of the photosensory module *Dr*BPhy in dark and light adapted states based on crystal structures refined against TRXSS data. The separation of the PHY domains is even more pronounced in the light adapted state than in the crystal structure and also the dark adapted state is a bit extended.

TRXSS measurements have also been performed for phytochromes from other bacteria [141]. The purpose was to investigate whether or not similar conformational rearrangements could be seen in different members of this protein family. The proteins investigated were the photosensory core of phytochromes Agp1 and Agp2 from *Agrobacterium tumefaciens*, where Agp1 is a canonical and Agp2 a non canonical phytochrome [113], P1 and P2 from *Stigmatella aurantiaca* as well as a tyrosine to histidine mutant of P1 that rescues the loss of photochromicity exhibited by wildtype P1 [142].

Interestingly, all of these phytochrome fragments showed highly similar red light-induced difference scattering pattern to that of *Dr*BPhy, indicating that they all undergo similar conformational rearrangements. This is especially interesting as it shows that for the bathy phytochrome Agp2, only the chromophore photocycle acts in reverse, whilst the global conformational rearrangements do not. The behaviour of P1 and the P1 Y$\rightarrow$H rescue mutant shows that complete photochromicity is not a prerequisite for global conformational rearrangements in response to light and shows the need for techniques complementary to absorption spectroscopy when studying signal transduction.

4.5 Modulation of the output domain

Ultimately, the structural signal has to modulate the activity of the output domain, which for many phytochromes is a histidine kinase (HK). Whether or not the output module of *Dr*BPhy is a HK is unclear. The output domain certainly shows sequence homology with other histidine kinases [123], but there is no conclusive evidence for kinase activity. In the interest of keeping things simple, and because sequence similarity would suggest a highly similar structure, I will regard the output module of *Dr*BPhy as a histidine kinase in this thesis.

There are no crystal structures available for the full length phytochrome, probably due to the internal flexibility of the HK domain or the flexibility between the HK and sensory domain. Studies using electron microscopy [143, 144] show how the HK is placed on top of the sensory module in the dark, but in the light it appears that in some of the micrographs the HK domain cannot be distinguished properly [143, 144]. The dramatic separation of the PHY domains of the photosensory module suggested that one possibility would be the complete separation of the two kinase monomers. Indeed, mutating a couple of residues at the GAF-GAF interface results in a protein where the HK-HK interface is broken in response to red light illumination [145]. On the other hand, there are several structures available for isolated HK domains which all show an intact HK dimer interface, regardless of whether or not the HK is in an active or inactive state [146]. In addition, a recent study on a different phytochrome, Agp1, using EPR showed no pronounced change in distance between subunits [147].

In **Paper II** we investigate the structure and structural activation of full length *Dr*BPhy using a combination of TRXSS and conventional SAXS (section 3.3). The limited data in a SAXS curve was sufficient to reconstruct the overall shape of the protein, approximately on a similar level of resolution as the electron micrographs in refs. [143, 144]. This analysis revealed a dark adapted state in which the photosensory module and a typical HK module can easily be docked (Figure 4.7). It is clear that the scattering data does not support a model where the HK dimer breaks apart upon light activation. Instead the HK domains appear to rotate with respect to the sensory module. At this resolution it is not possible to say

whether the HK rotates completely or whether it rearranges internally, but reorientation of the CA domains on the DHp helices have been suggested as an important conformational change in HK regulation [146, 148].

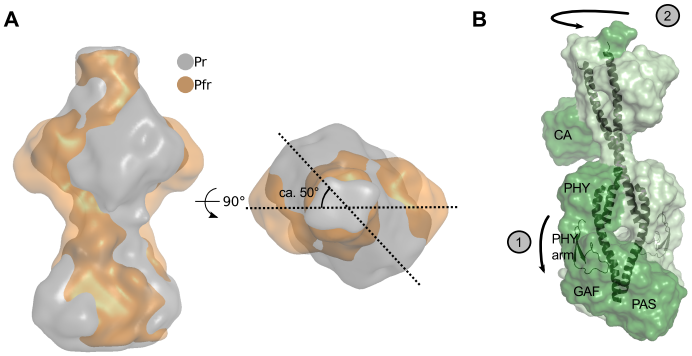

Figure 4.7: SAXS derived envelopes of full length *Dr*BPhy. (A) Envelopes of the dark and light adapted *Dr*BPhy reveals a rotation of the HK module with respect to the sensory module. (B) Light absorption causes the refolding of the PHY arm (1) and the rotation of the kinase domain (2).

4.6 Summary

Using TRXSS we probed the structural photoactivation and signal transduction in *Dr*BPhy. This work has resulted in **Paper I** and **II** and revealed that the photoactivation of the photosensory core module involves the refolding of the PHY-arm as well as the separation of the PHY domains. The large light-induced separation of the PHY domains may be an artifact of the truncation and is likely smaller in the full-lenght protein. The PHY domain separation feeds into the HK output domain, causing the apparent rotation of the entire domain. All these events happen within milliseconds of light absorption suggesting that the chromophore is in the transition between meta-Ra and meta-Rc. This transition has previously been associated with a deprotonation reaction, which may be the ultimate trigger of the structural photoactivation of *Dr*BPhy.

Chapter 5

Photoreceptors with light-oxygen-voltage domains

In **Paper III** and **IV** we investigated the blue light sensing photoreceptors that contain a Light-Oxygen-Voltage (LOV) domain. These proteins mediate diverse processes such as phototropism in plants [149], DNA binding [150], and virulence and stress response in bacteria [151, 152]. The photosensory core of a LOV photoreceptor is the LOV photosensor domain. The domains can be functionally coupled to a wide range of transducer and effector domains [153]. The inherent modularity of LOV receptors also makes them prime candidates for the construction of genetically encoded light-sensitive proteins [154].

5.1 LOV domain structure.

The first LOV domain structure solved was that of *Adiantum capillus-veneris* neochrome 1 [155]. The structure can be seen in Figure 5.1 and comprises five anti parallel β-strands and four α-helices and has structural homology with the widespread Per-Arnt-Sim (PAS) sensory domain. The flavin chromophore is wedged between the β-sheet and helices Eα and Fα. In many cases the LOV core domain is flanked by α-helices or β-strands. These are important for signal transduction and will be further discussed in section 5.3.

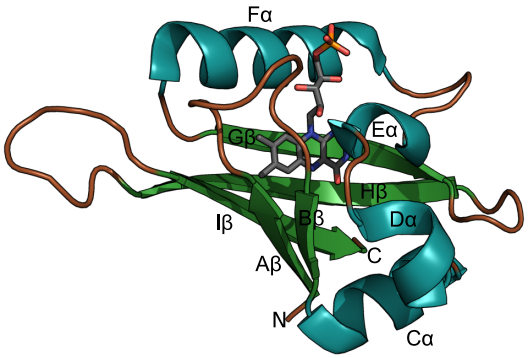

Figure 5.1: LOV domain structure. The structure of LOV2 domain from *Adiantum capillus-veneris* neochrome 1 (pdb id: 1G28).

5.2 LOV domain photochemistry.

A flavin chromophore, usually flavin mononucleotide, resides within the LOV domain. This chromophore is responsible for the absorption of blue light around 450 nm [156–158]. The primary photochemical events have been elucidated primarily using absorption spectroscopy. A photon is absorbed by the dark-adapted state (FMN^{A450}), forming an excited flavin singlet state (FMN^{*}) on a picosecond timescale (Figure 5.2) [159]. This state decays into a triplet state (FMN^{T}) over several nanoseconds [160]. Within microseconds a covalent thioadduct (FMN^{A390}) is formed between the flavin atom C4a and a conserved cysteine residue of the LOV photosensor [161], likely via a radical intermediate. Depending on the chromophore environment, temperature, and solvent conditions the flavin-cysteinyl adduct is stable for several seconds, minutes or even hours [158]. Along with adduct formation, the

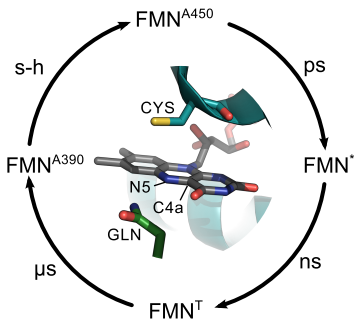

Figure 5.2: LOV domain photocycle. The canonical photocycle of an FMN chromophore within a LOV domain, with the FMN chromophore in its binding pocket.

flavin N5 nitrogen is protonated [19, 159]. Recent studies show that N5 protonation, rather than thioadduct formation, is required for signal transduction [162]. N5 protonation causes the rotation of a nearby conserved glutamine residue further relaying the signal [163–165].

5.3 Signal transducing elements in LOV photoreceptors.

While the LOV photochemistry is well understood, and the vast majority of LOV receptors exhibit the same photochemistry. The way in which these events are relayed through the protein are not as conserved [158, 166, 167]. Depending on the protein architecture, LOV activation can result in dimerization [168] or monomerization [169] of the entire photoreceptor protein, or it can lead to repositioning of the LOV domains [170]. A closer look shows that all these different signaling modes are similar in one aspect; LOV activation modifies a binding site on the surface of a β-sheet adjacent to the chromophore. This binding site can be occupied by the C-terminal Jα helix, the N-terminal extension, or the A'α helix. This is exemplified by the structures of *Avena sativa* (oat) phototropin 1 [171] (Figure 5.3), VIVID from the fungus *Neurospora crassa* [165, 168] and aureochrome 1a from the diatom *Phaeodactylum tricornutum* [170]. In all these cases, photoactivation of the LOV domain leads to dissociation of the bound element.

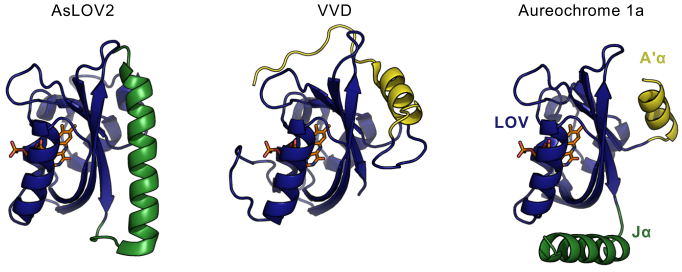

Figure 5.3: Signal transduction in LOV domains. LOV domains and the flanking signal transducing elements for *As*LOV2 (pdb id: 2V0U), *Nc*VVD (pdb id: 2PD7) and aureochrome 1a (pdb id: 5DKK).

5.4 Structural photoactivation of the YtvA-LOV domain

In **Paper III** we investigated the structural photoactivation of the LOV domain from *Bacillus subtilis* YtvA (*Bs*YtvA). Next to the three modes of signal transduction mentioned in section 5.3, this dimeric protein represents yet another signaling strategy. Each monomer of *Bs*YtvA consists of a LOV domain, an α-helical linker denoted Jα, and a Sulfate Transporter and Anti-Sigma factor antagonist (STAS) domain. The structures of both the dark and light adapted form of *Bs*YtvA (lacking the STAS domain) were solved already about 10 years ago [164]. This study suggested a minute light-induced rotation of the two LOV domains, with respect to each other. Because the crystallized construct was lacking the N-terminal A'α helix, which can be expected to be important for signal transduction as mentioned in section 5.3, the relevance of these findings may be questioned. Later the light-gated histidine kinase YF1 was engineered based on *Bs*YtvA [172] and when the structure of this protein was solved by crystallography [25] it displayed a completely different interface between the two LOV monomers (Figure 5.4). Specifically the A'α helix of the neighboring monomer occupies the binding site on the β-sheet opposite the chromophore, thus entangling the two monomers.

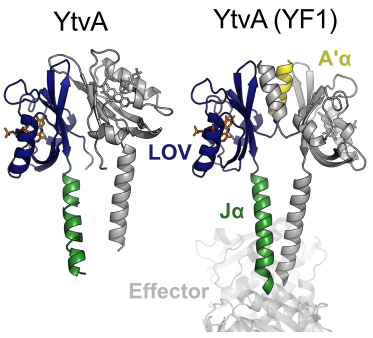

Figure 5.4: structure of *Bs*YtvA. LOV domains and the Jα-helix of *Bs*YtvA in the construct lacking A'α (pdb id: 2PR5), and as present in YF1 (pdb id: 4GCZ).

In a TRXSS experiment we detected global conformational rearrangements about 2 µs after laser exposure (Figure 5.5). This is the same time as the formation of the flavin-cysteinyl adduct [173]. The Fourier sine transform of the data suggested a light-induced separation of the

two monomers. More extensive structural modeling based on TRXSS-filtered MD simulations revealed that this indeed was the case. The LOV monomers splay apart at the connection site of the Jα -helix, whilst the A'α domains hardly move at all (Figure 5.5D).

The maximal separation was only about 3 Å, therefore it was very reassuring to see that an EPR study revealed the very same conformational change, in the context of full-length YF1 [174]. We compared the light-induced changes refined against TRXSS data to those found in the crystal structure [164]. Despite the lack of the A'α helix much of the changes are in qualitative agreement. Apparently the essence of the light-induced conformational changes are encoded within the LOV domain core, but the A'α helices are necessary for amplification of this signal.

It is also interesting to note that the conformational change in *Bs*YtvA-LOV is qualitatively similar to that found in the *Dr*BPhy photosensory module, but about ten times smaller in magnitude. It appears plausible that light-induced splaying apart of dimeric sensory domains may be a general strategy for signal transduction.

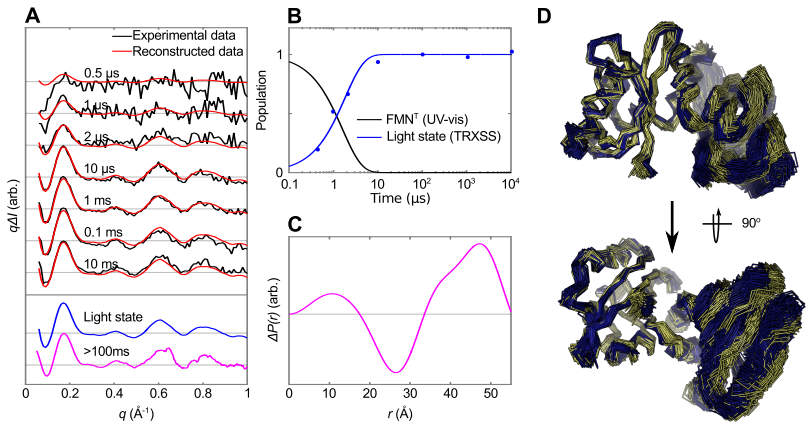

Figure 5.5: TRXSS data and refined conformational changes for *Bs*YtvA-LOV. (A) A difference signal appears about 2 µs after light absorption and remains for several seconds. (B) The rise of the signal is simultaneous with the formation of the chromophore photoproduct state. (C) The corresponding change in *P(r)*. (D) The refined conformational change, dark state shown in blue and light state in yellow. Adapted from **Paper III**.

5.5 Signal transduction and modulation of the effector domain

We also collected scattering data for full-length YF1. This revealed, like for the sole sensory domain, conformational rearrangements following the formation of the photoproduct state at about 2 µs (Figure 5.6). In addition the data also revealed a second conformational transition at about 250 ms. This was something that had not been observed in *Bs*YtvA-LOV alone, suggesting that the secondary change was mainly localized to the HK output domain. Structural refinement against the scattering data revealed a left-handed rotation of the output domain with respect to the kinase domain. Additionally, the secondary state showed rearrangements within the output domain, specifically it appeared that the CA domains rearrange on the DHp domains.

This is only one set of models that agrees with the data, and there may be other ones which we did not observe. However, the model that we propose is in agreement with the current understanding of SHK regulation. The structure of YF1 reveals a coiled-coil forming between the two Jα-helices [25]. Coiled-coils are well known signal transducing elements found in for example the thermosensor DesK [175] and HAMP domains [176]. The 3 Å photo induced separation at the base of the Jα-helices identified for *Bs*YtvA-LOV ought lead to an increased left-handed supercoiling of the Jα-helices. Previous work has, through biochemical assays, established that the angular orientation of the helices in the linker region is of paramount importance for signal transduction in YF1 [177], further suggesting that it is a change of the supercoiling that is regulating the kinase activity. The left-handed supercoiling is also in agreement with biochemical [176] and structural data [29] for other systems.

A model in which increased separation at the base of the Jα-helices causes increased *left-handed* supercoiling also provides a rationale for the inverted signal polarity of a YF1 mutant [25]. In a parallel study, this mutant was investigated by EPR [174]. This investigation revealed an altered dimer interface in the sensory domain, nevertheless the two monomers splay apart in response to light also in this case. An explanation, in line

with our proposed model, is that light in this case causes *right-handed* supercoiling. Although supported by current data, this explanation is rather speculative at the moment.

The second phase of structural rearrangement that is localized to the HK domain is also in agreement with the general understanding of HK regulation. Studies have shown that the positioning of the CA domains on the DHp helices are important for HK activation [146, 148, 178]. Because many photoreceptors are constructed based on modular principles, where a selection of sensory domains can be coupled to a variety of effector domains [179], it is possible that the mode of regulation revealed in **Paper IV** will be found in several photoreceptors.

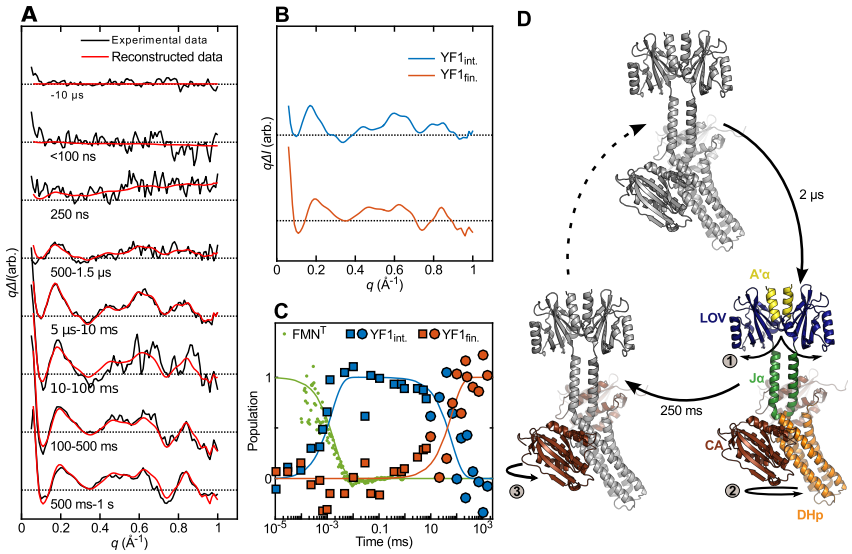

Figure 5.6: TRXSS data and light-induced conformational changes in YF1. (A) A difference signal appears about 2 µs after light absorption. (B) Two states are sufficient to reproduce the data. (C) The first conformational transition occurs simultaneously with the formation of the chromophore photoproduct state, after ca. 250 ms another conformational transition occurs. (D) Absorption of light causes the sensory domain to splay apart, resulting in supercoiling of the α-helical linker and the rotation of the output domain. A secondary structural transition involves the repositioning of the CA domains on the DHp domain. Adapted from **Paper IV**.

5.6 Summary

Using TRXSS we show that the absorption of blue light causes the two monomers of *Bs*YtvA-LOV to splay apart by ca. 3 Å, simultaneously with the formation of the flavin-cysteinyl photoadduct state. In YF1, this separation feeds into the connecting Jα-helices causing a left handed supercoiling, that alters the binding mode of the CA domains on the DHp domains. After about 250 ms the CA domains rearrange on the DHp domain, thereby modulating the activity of the kinase output domain.

Chapter 6

Cryptochromes

In **Paper V** we examined a member of the cryptochrome family, specifically the cryptochrome from *Drosophila melanogaster* (*Dm*Cry). Cryptochromes are blue light sensing photoreceptors that were initially discovered in *Arabidopsis thaliana* [180] and have since been found in most higher plants and animals but only in a few prokaryotes [181].

Cryptochromes have about 45% sequence similarity and a high structural similarity with photolyases, a family of proteins that repair UV-damaged DNA using light energy [182]. Compared to photolyases, cryptochromes have no, or very little DNA repair abilities and are mainly functioning as photoreceptors [149]. Cryptochromes provide light signals to the circadian clock [183, 184] and may also function as magnetosensors [185].

*Dm*Cry is a type I insect cryptochrome, meaning that it is primarily a photoreceptor. In *D. melanogaster* it is a main component of the circadian clock and it coordinates interactions between Timeless (TIM) and the E3-ubiquitin ligase Jetlag (JET) [183, 184, 186, 187].

6.1 Cryptochrome structure

The three dimensional structure of cryptochromes is highly similar to that of the DNA repair enzyme photolyase (Figure 6.1) [188–190]. The protein consist of two globular domains, one assuming the so called Rossman fold, with both helix and sheet structures (α/β domain) and one that is only helical (helical domain). There is a cleft between α/β domain and the helical domain. In a subfamily of cryptochromes known as DASH-cryptochromes,

this cleft has been shown to bind a folate antenna cofactor [191], but no such binding was observed in *Dm*Cry [192].

The helical domain holds a FAD chromophore responsible for light absorption. The two domains are connected by a linking region that is different in photolyases compared to cryptochromes. A region called the phosphate binding loop also adopts different confirmation in the solved cryptochrome and photolyase structures [192, 193]. Interestingly, if a part of the so called protrusion motif is deleted, the phosphate binding loop in *Dm*Cry adopts a position similar to that found in photolyases. Cryptochromes also have an extension at their carboxy-terminus, called the CTT (C-terminal tail), that is not found in photolyases. In fact, the CTT in cryptochromes occupy the region that in photolyases is the DNA binding pocket. Specifically, it is phenylalanine 534 of the conserved FFW motif that takes the place of the DNA substrate [192, 194, 195]. The length of the CTT varies between organisms and can be several hundred residues long [181]. In *Dm*Cry the CTT consists of about 50 residues [192, 195].

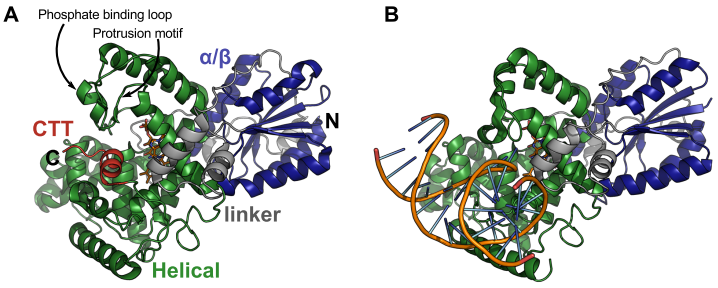

Figure 6.1: Cryptochrome structure. (A) Overall structure of cryptochromes (pdb id: 4GU5). The α/β domain shown in blue, the linking region in gray, the helical domain in green and the CTT in red. (B) Overall architecture of photolyases, here represented by *Drosophila* 6-4 photolyase (pdb id: 3CVY).

6.2 Cryptochrome photochemistry

The FAD chromophore found in cryptochromes can adopt a range of different redox states. In plant cryptochromes the FAD exists in the oxidized form in the dark. In response to light the neutral semiquinone radical ($FADH^{\bullet}$) is formed [149]. In animal cryptochromes such as *Dm*Cry the FAD is purified in the oxidized state and forms an anion radical ($FAD^{\bullet-}$) in response to light. There has been some debate as to what is the resting and signaling state of *Dm*Cry [196,197], but over the last years the literature is converging towards the model with the oxidized flavin in the resting state and $FAD^{\bullet-}$ in the signaling state. Recent studies have also pointed out that even if *Dm*Cry mostly forms $FAD^{\bullet-}$ under constant illumination, it also forms a small amount of $FADH^{\bullet}$ [198, 199].

Blue light exposure of the FAD triggers electron transfer along a series of tryptophan residues [149] (Figure 6.2). In plant cryptochromes this is a conserved triad of tryptophan residues, whilst it in animal cryptochromes a fourth tryptophan was recently discovered [199,200]. The electron transport along the four tryptophan residues (Trp_A-Trp_D, in *DmCry* Trp420, Trp397, Trp342, Trp394) is fast and finished within a few nanoseconds. On a microsecond timescale Trp_D is deprotonated [201]. The oxidized state of the chromophore is recovered by reoxidation by oxygen or another electron acceptor such as ferricyanide.

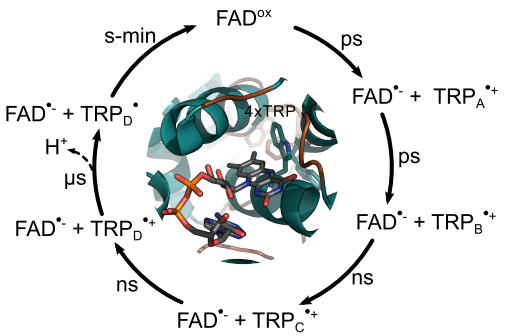

Figure 6.2: Cryptochrome photocycle. FAD photochemistry in animal cryptochromes.

6.3 Signal transduction in cryptochromes*

Using limited proteolysis, SAXS [202] and transient grating [203] it has been suggested that the final event of cryptochrome structural photoactivation is the undocking or unstructuring of the CTT. This enables interaction with downstream proteins, presumably by exposing a new interaction surface. Consistent with this interpretation, ΔCTT mutants appear constitutively active [197]. The FFW motif in the CTT has also been shown to be of great importance for the correct functioning of *Dm*Cry [202].

There is little detail on the structural events that follow photon absorption and ultimately lead to CTT release. In between the FAD and the CTT lies a highly conserved histidine residue. In *Dm*Cry this is His378. In photolyases a histidine residue at the equivalent position has been shown to be a prerequisite for DNA repair [204, 205] and light-induced conformational changes [206]. A recent mutational and computational study revealed that exchanging His378 in *Dm*Cry for large charged residues destabilizes the CTT and makes it more accessible to proteases [198]. The authors could also see that in the dark His378 was most likely singly protonated and that flavin reduction promoted the formation of the doubly protonated form. This caused a changed position of His378, which effectively pushed on the FFW motif and caused the CTT to undock.

In **Paper V** we used TRXSS to investigate what overall conformational rearrangements are involved in signal transduction, and experimentally assess whether His378 is involved. In the experiment we examined wildtype *Dm*Cry as well as a histidine to alanine mutant, *Dm*Cry H378A. Additionally, the experiment was conducted at two different pH, at pH 7 and at pH 9. If the protonation of His378 is involved, altering the pH should in some way inhibit the formation of the signaling state.

These experiments revealed the existence of several structural intermediates and up to four species, termed *Dm*Cry$_\alpha$-*Dm*Cry$_\delta$, were needed explain the data (Figure 2 of **Paper V**). Conformational transitions were observed at ca. 2.5-6 µs, 420 µs, and at 2.5 ms. The final state (*Dm*Cry$_\delta$) showed remarkable similarity to the steady state difference scattering (Figure 3 of **Paper V** and ref. [202]), suggesting that this is the signaling state

*This section describes unpublished work and the primary data are therefore not reproduced. Instead, the text refers to figures in the attached manuscript, Paper V.

with an undocked CTT. Interestingly, both the wildtype and the H378A mutant form this state. This is a clear indication that His378 is not a crucial residue for signal transduction in *Dm*Cry. In addition, the formation of *Dm*Cry$_\delta$ can only be seen at pH 7 and not at pH 9. This would suggest that some residue needs to be protonated before the final conformational transition.

Through the use of MD simulations we were able to propose a function for the conserved His378. In the dark, when FAD is oxidized, His378 forms a hydrogen bond to Trp536 in the FFW motif (Figure 6.3A). This prevents the CTT from detaching and thus stabilizes the dark adapted state. When FAD is photoreduced to FAD$^{\bullet-}$, His378 instead binds to the chromophore, thereby releasing the CTT (Figure 6.3B). As His378 is mutated to an alanine the CTT is less stable in general and in one trajectory it departed completely, despite the chromophore being in its dark state. This is an indication that the main purpose of His378 is to stabilize the dark adapted structure of *Dm*Cry.

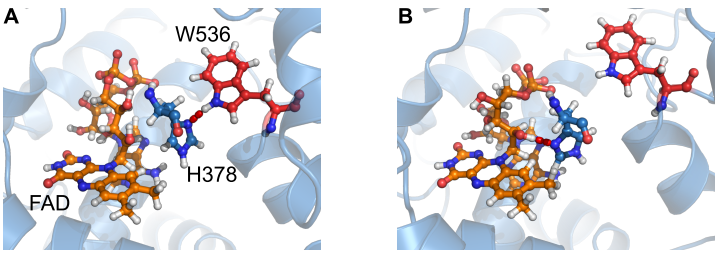

Figure 6.3: Hydrogen bonding network around FAD. (A) In the dark His378 forms a hydrogen bond to Trp536. (B) After light absorption this is disrupted and His378 instead binds to the FAD chromophore. Adapted from **Paper V**

The results of **Paper V** lead us to propose a sequence of events in *Dm*Cry photoactivation (Figure 6.4). In the dark His378 forms a hydrogen bond with Trp536, thereby keeping the CTT fully attached. Light absorption by the FAD triggers electron transfer along the tryptophan tetrad. This leads to the formation of a positively charged tryptophan radical at Trp$_\mathrm{D}$ (Trp394) [201]. This residue is close to the surface and the altered surface charge cause an increased density of the hydration shell (*Dm*Cry$_\alpha$). The density of the solvation layer decreases as Trp$_\mathrm{D}$ is

deprotonated (*Dm*Cry$_\beta$). Flavin reduction also causes His378 to break the hydrogen bond to Trp536. This renders the CTT more flexible and results in a local decrease in the hydration layer density around the CTT (*Dm*Cry$_\gamma$). The more flexible CTT still remains within or close to its binding pocket until the protonation of some residue causes it to release completely (*Dm*Cry$_\delta$).

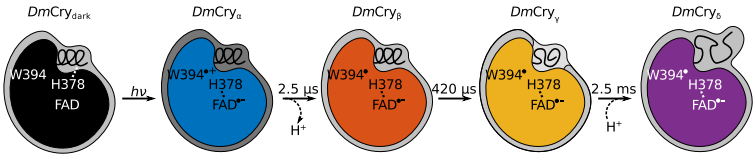

Figure 6.4: Proposed photoactivation of *Dm*Cry. A schematic representation of the main events during the photoactivation of *Dm*Cry.

6.4 Summary

By combining all atom MD simulations and TRXSS in **Paper V** we are able to resolve the global conformational rearrangements in *Dm*Cry following photoexcitation. In addition we are able to propose that the main role of His378 is to stabilize the dark adapted state of the protein, and that complete structural photoactivation hinges on the protonation state of some residue.

Chapter 7

Concluding remarks

All the work in this thesis has in different ways made use of time-resolved X-ray solution scattering to investigate how the energy of a photon is converted into conformational rearrangements in different photoreceptor proteins. The investigated proteins differ in which wavelength is absorbed as well as size and oligomeric state. The length scale of the investigated conformational rearrangements have varied from sub Ångström to nanometer scale and the time range from a few nanoseconds to several hundreds of milliseconds.

It is evident that, in many ways, TRXSS is a fantastic technique for studying conformational changes and signal transduction in for example photoreceptor proteins. It is a direct structural probe (a highly sensitive one), solution based, requires no labeling, and it is possible to predict the scattering from atomic coordinates. One of the drawbacks of the method is no doubt the limited information. Because of this it is important that any detailed structural models are validated by additional data. In **Paper I** this was achieved by comparing them with a crystal structure, in **Paper III** the results were validated by comparing to those obtained by EPR, in **Paper IV** they were corroborated by biochemical assays and in **Paper V** we used the limited information from TRXSS to guide the interpretation of MD simulations. In **Paper II** the structural models are more global an qualitative. Therefore there is not as high a risk of over fitting the data.

By combining absorption spectroscopy and TRXSS it is possible to investigate both the local environment of the chromophore as well as the global conformation of photoactive proteins. I believe that *inline* and *online* combinations with for example absorption spectroscopy could be

greatly beneficial to TRXSS experiments. This would in several ways be preferable to performing separate sets of experiments, each with their own uncertainties, and afterwards attempt to correlate the results. Combinations with other structural techniques such as EPR or NMR should also be further investigated, as even sparse structural restraints would greatly aid the interpretation of the scattering data.

The detailed analysis of TRXSS data relies on the ability to efficiently and accurately calculate the scattering pattern from atomic coordinates. The software available today is either predominantly fast (eg. *CRYSOL* [35] or FoXS [38]) or accurate (eg. WAXSiS [39]). For much of the analysis sufficient speed is an absolute necessity, rendering the more accurate methods virtually unusable. MD simulations provide valuable information on an atomistic scale and are likely going to be (and should be) a major part of the TRXSS data analysis [108, 207, 208] but this too needs to be explored further.

Photoreceptor and generally photosensory proteins account for only a small part of the proteome and if TRXSS is to succeed as a general technique it needs to be able to target other proteins as well [209]. One of the main challenges will no doubt be the triggering of the reaction. Currently there are microfluidic devices available that can mix solutions of protein and for example a ligand in a few microseconds. In this case an additional challenge will be to either prepare huge amounts of sample as it can only be used once, or to devise strategies to reuse the sample. Another idea is to induce conformational changes using infrared [210] or terahertz radiation [211] or electrical fields [212]. In these cases, extreme care must be taken to ensure that the triggered conformational changes are relevant, and not just an artifact of the excitatory method.

If these obstacles can be overcome and advances are made towards more general ways of structural interpretation of the data, I can definitely see TRXSS as a widely applicable and complementary technique for studying protein dynamics.

Bibliography

[1] J. C. Kendrew, G. Bodo, H. M. Dintzis, R. G. Parrish, H. Wyckoff, and D. C. Phillips, "A three-dimensional model of the myoglobin molecule obtained by x-ray analysis.," *Nature*, vol. 181, pp. 662–6, 3 1958.

[2] A. Ansari, J. Berendzen, S. F. Bowne, H. Frauenfelder, I. E. Iben, T. B. Sauke, E. Shyamsunder, and R. D. Young, "Protein states and proteinquakes.," *Proceedings of the National Academy of Sciences of the United States of America*, vol. 82, pp. 5000–4, 8 1985.

[3] K. Henzler-Wildman and D. Kern, "Dynamic personalities of proteins.," *Nature*, vol. 450, pp. 964–72, 12 2007.

[4] U. Hensen, T. Meyer, J. Haas, R. Rex, G. Vriend, and H. Grubmüller, "Exploring protein dynamics space: the dynasome as the missing link between protein structure and function.," *PloS one*, vol. 7, no. 5, p. e33931, 2012.

[5] P. Debye, "Interferenz von Röntgenstrahlen und Wärmebewegung," *Annalen der Physik*, vol. 348, no. 1, pp. 49–92, 1913.

[6] I. Waller, "Zur Frage der Einwirkung der Wärmebewegung auf die Interferenz von Röntgenstrahlen," *Zeitschrift für Physik*, vol. 17, pp. 398–408, 12 1923.

[7] H. Frauenfelder, G. A. Petsko, and D. Tsernoglou, "Temperature-dependent X-ray diffraction as a probe of protein structural dynamics.," *Nature*, vol. 280, no. 5723, pp. 558–563, 1979.

[8] V. Srajer, Z. Ren, T. Y. Teng, M. Schmidt, T. Ursby, D. Bourgeois, C. Pradervand, W. Schildkamp, M. Wulff, and K. Moffat, "Protein conformational relaxation and ligand migration in myoglobin: a nanosecond to millisecond molecular movie from time-resolved Laue X-ray diffraction.," *Biochemistry*, vol. 40, pp. 13802–13815, 11 2001.

[9] H. Ihee, S. Rajagopal, V. Srajer, R. Pahl, S. Anderson, M. Schmidt, F. Schotte, P. a. Anfinrud, M. Wulff, and K. Moffat, "Visualizing reaction pathways in photoactive yellow protein from nanoseconds to seconds.," *Proceedings of the National Academy of Sciences of the United States of America*, vol. 102, no. 1, pp. 7145–7150, 2005.

[10] R. Aranda, E. J. Levin, F. Schotte, P. A. Anfinrud, and G. N. Phillips, "Time-dependent atomic coordinates for the dissociation of carbon monoxide from myoglobin.," *Acta crystallographica. Section D, Biological crystallography*, vol. 62, pp. 776–83, 7 2006.

[11] X. Yang, Z. Ren, J. Kuk, and K. Moffat, "Temperature-scan cryocrystallography reveals reaction intermediates in bacteriophytochrome.," *Nature*, vol. 479, pp. 428–32, 10 2011.

[12] T. R. M. Barends, L. Foucar, A. Ardevol, K. Nass, A. Aquila, S. Botha, R. B. Doak, K. Falahati, E. Hartmann, M. Hilpert, M. Heinz, M. C. Hoffmann, J. Köfinger, J. E. Koglin, G. Kovacsova, M. Liang, D. Milathianaki, H. T. Lemke, J. Reinstein, C. M. Roome, R. L. Shoeman, G. J. Williams, I. Burghardt, G. Hummer, S. Boutet, and I. Schlichting, "Direct observation of ultrafast collective motions in CO myoglobin upon ligand dissociation.," *Science (New York, N.Y.)*, vol. 350, pp. 445–50, 10 2015.

[13] X. Zeng, Z. Ren, Q. Wu, J. Fan, P.-P. Peng, K. Tang, R. Zhang, K.-H. Zhao, and X. Yang, "Dynamic Crystallography Reveals Early Signalling Events in Ultraviolet Photoreceptor UVR8.," *Nature plants*, vol. 1, no. January, p. 14006, 2015.

[14] E. Nango, A. Royant, M. Kubo, T. Nakane, C. Wickstrand, T. Kimura, T. Tanaka, K. Tono, C. Song, R. Tanaka, T. Arima, A. Yamashita, J. Kobayashi, T. Hosaka, E. Mizohata, P. Nogly, M. Sugahara, D. Nam, T. Nomura, T. Shimamura, D. Im, T. Fujiwara, Y. Yamanaka, B. Jeon, T. Nishizawa, K. Oda, M. Fukuda, R. Andersson, P. Båth, R. Dods, J. Davidsson, S. Matsuoka, S. Kawatake, M. Murata, O. Nureki, S. Owada, T. Kameshima, T. Hatsui, Y. Joti, G. Schertler, M. Yabashi, A.-N. Bondar, J. Standfuss, R. Neutze, and S. Iwata, "A three-dimensional movie of structural changes in bacteriorhodopsin.," *Science (New York, N.Y.)*, vol. 354, no. 6319, pp. 1552–1557, 2016.

[15] S. Bandara, Z. Ren, L. Lu, X. Zeng, H. Shin, K.-H. Zhao, and X. Yang, "Photoactivation mechanism of a carotenoid-based photoreceptor.," *Proceedings of the National Academy of Sciences of the United States of America*, vol. 114, pp. 6286–6291, 6 2017.

[16] M. Suga, F. Akita, M. Sugahara, M. Kubo, Y. Nakajima, T. Nakane, K. Yamashita, Y. Umena, M. Nakabayashi, T. Yamane, T. Nakano, M. Suzuki, T. Masuda, S. Inoue, T. Kimura, T. Nomura, S. Yonekura, L.-J. Yu, T. Sakamoto, T. Motomura, J.-H. Chen, Y. Kato, T. Noguchi, K. Tono, Y. Joti, T. Kameshima, T. Hatsui, E. Nango, R. Tanaka, H. Naitow, Y. Matsuura, A. Yamashita, M. Yamamoto, O. Nureki, M. Yabashi, T. Ishikawa, S. Iwata, and J.-R. Shen, "Light-induced structural changes and the site of O=O bond formation in PSII caught by XFEL.," *Nature*, vol. 543, no. 7643, pp. 131–135, 2017.

[17] J. A. McCammon, B. R. Gelin, and M. Karplus, "Dynamics of folded proteins," *Nature*, vol. 267, pp. 585–590, 6 1977.

[18] J. Dasgupta, R. R. Frontiera, K. C. Taylor, J. C. Lagarias, and R. A. Mathies, "Ultrafast excited-state isomerization in phytochrome revealed by femtosecond stimulated Raman spectroscopy.," *Proceedings of the National Academy of Sciences of the United States of America*, vol. 106, pp. 1784–9, 2 2009.

[19] T. Kottke, J. Heberle, D. Hehn, B. Dick, and P. Hegemann, "Phot-LOV1: photocycle of a blue-light receptor domain from the green alga Chlamydomonas reinhardtii.," *Biophysical journal*, vol. 84, pp. 1192–201, 2 2003.

[20] T. Biskup, K. Hitomi, E. D. Getzoff, S. Krapf, T. Koslowski, E. Schleicher, and S. Weber, "Unexpected electron transfer in cryptochrome identified by time-resolved EPR spectroscopy.," *Angewandte Chemie (International ed. in English)*, vol. 50, pp. 12647–51, 12 2011.

[21] R. Gao and A. M. Stock, "Biological insights from structures of two-component proteins.," *Annual review of microbiology*, vol. 63, pp. 133–54, 2009.

[22] P. M. Wolanin, P. A. Thomason, and J. B. Stock, "Histidine protein kinases: key signal transducers outside the animal kingdom.," *Genome biology*, vol. 3, p. REVIEWS3013, 9 2002.

[23] M. Goulian, "Two-component signaling circuit structure and properties.," *Current opinion in microbiology*, vol. 13, pp. 184–9, 4 2010.

[24] C. Wang, J. Sang, J. Wang, M. Su, J. S. Downey, Q. Wu, S. Wang, Y. Cai, X. Xu, J. Wu, D. B. Senadheera, D. G. Cvitkovitch, L. Chen, S. D. Goodman, and A. Han, "Mechanistic insights revealed by the crystal structure of a histidine kinase with signal transducer and sensor domains.," *PLoS biology*, vol. 11, p. e1001493, 1 2013.

[25] R. P. Diensthuber, M. Bommer, T. Gleichmann, and A. Möglich, "Full-length structure of a sensor histidine kinase pinpoints coaxial coiled coils as signal transducers and modulators.," *Structure (London, England : 1993)*, vol. 21, pp. 1127–36, 7 2013.

[26] P. Casino, V. Rubio, and A. Marina, "Structural insight into partner specificity and phosphoryl transfer in two-component signal transduction.," *Cell*, vol. 139, pp. 325–36, 10 2009.

[27] P. Casino, L. Miguel-Romero, and A. Marina, "Visualizing autophosphorylation in histidine kinases.," *Nature communications*, vol. 5, p. 3258, 1 2014.

[28] J. W. Willett, J. Herrou, A. Briegel, G. Rotskoff, and S. Crosson, "Structural asymmetry in a conserved signaling system that regulates division, replication, and virulence of an intracellular pathogen.," *Proceedings of the National Academy of Sciences of the United States of America*, vol. 112, pp. 3709–3718, 7 2015.

[29] F. Trajtenberg, J. A. Imelio, M. R. Machado, N. Larrieux, M. A. Marti, G. Obal, A. E. Mechaly, and A. Buschiazzo, "Regulation of signaling directionality revealed by 3D snapshots of a kinase:regulator complex in action.," *eLife*, vol. 5, 12 2016.

[30] B. E. Warren, *X-ray Diffraction*. Courier Corporation, 1969.

[31] D. I. Svergun, M. V. Petoukhov, and M. H. Koch, "Determination of domain structure of proteins from X-ray solution scattering.," *Biophysical journal*, vol. 80, pp. 2946–53, 6 2001.

[32] P. Debye, "Zerstreuung von Röntgenstrahlen," *Annalen der Physik*, vol. 351, no. 6, pp. 809–823, 1915.

[33] W. H. Bragg and W. L. Bragg, "The Reflection of X-rays by Crystals," *Proceedings of the Royal Society A: Mathematical, Physical and Engineering Sciences*, vol. 88, pp. 428–438, 7 1913.

[34] F. Merzel and J. C. Smith, "Is the first hydration shell of lysozyme of higher density than bulk water?," *Proceedings of the National Academy of Sciences of the United States of America*, vol. 99, no. 8, pp. 5378–5383, 2002.

[35] D. Svergun, C. Barberato, and M. H. Koch, "CRYSOL - A program to evaluate X-ray solution scattering of biological macromolecules from atomic coordinates," *Journal of applied crystallography*, vol. 28, no. 6, pp. 768–773, 1995.

[36] J. Bardhan, S. Park, and L. Makowski, "SoftWAXS: a computational tool for modeling wide-angle X-ray solution scattering from biomolecules.," *Journal of applied crystallography*, vol. 42, pp. 932–943, 10 2009.

[37] H. Liu, R. J. Morris, A. Hexemer, S. Grandison, and P. H. Zwart, "Computation of small-angle scattering profiles with three-dimensional Zernike polynomials.," *Acta crystallographica. Section A, Foundations of crystallography*, vol. 68, pp. 278–85, 3 2012.

[38] D. Schneidman-Duhovny, M. Hammel, and A. Sali, "FoXS: a web server for rapid computation and fitting of SAXS profiles.," *Nucleic acids research*, vol. 38, pp. 540–4, 7 2010.

[39] C. J. Knight and J. S. Hub, "WAXSiS: a web server for the calculation of SAXS/WAXS curves based on explicit-solvent molecular dynamics.," *Nucleic acids research*, vol. 43, pp. 225–30, 7 2015.

[40] D. K. Putnam, E. W. Lowe, and J. Meiler, "Reconstruction of SAXS Profiles from Protein Structures.," *Computational and structural biotechnology journal*, vol. 8, p. e201308006, 8 2013.

[41] H. B. Stuhrmann, "Interpretation of small-angle scattering functions of dilute solutions and gases. A representation of the structures related to a one-particle scattering function," *Acta Crystallographica Section A*, vol. 26, pp. 297–306, 5 1970.

[42] R. D. B. Fraser, T. P. MacRae, and E. Suzuki, "An improved method for calculating the contribution of solvent to the X-ray diffraction pattern of biological molecules," *Journal of applied crystallography*, vol. 11, pp. 693–694, 12 1978.

[43] T. M. Raschke, "Water structure and interactions with protein surfaces," *Current opinion in structural Biology*, vol. 16, no. 2, pp. 152–159, 2006.

[44] J. D. Nickels, H. O'Neill, L. Hong, M. Tyagi, G. Ehlers, K. L. Weiss, Q. Zhang, Z. Yi, E. Mamontov, J. C. Smith, and A. P. Sokolov, "Dynamics of protein and its hydration water: neutron scattering studies on fully deuterated GFP.," *Biophysical journal*, vol. 103, pp. 1566–75, 10 2012.

[45] J. H. Roh, J. E. Curtis, S. Azzam, V. N. Novikov, I. Peral, Z. Chowdhuri, R. B. Gregory, and A. P. Sokolov, "Influence of hydration on the dynamics of lysozyme.," *Biophysical journal*, vol. 91, pp. 2573–88, 10 2006.

[46] A. C. Fogarty and D. Laage, "Water dynamics in protein hydration shells: the molecular origins of the dynamical perturbation.," *The journal of physical chemistry. B*, vol. 118, pp. 7715–29, 7 2014.

[47] L. Biedermannová and B. Schneider, "Hydration of proteins and nucleic acids: advances in experiment and theory. A review," *BBA - General Subjects*, vol. 1860, no. 9, pp. 1821–1835, 2016.

[48] M. H. Koch, P. Vachette, and D. I. Svergun, "Small-angle scattering: a view on the properties, structures and structural changes of biological macromolecules in solution.," *Quarterly reviews of biophysics*, vol. 36, pp. 147–227, 5 2003.

[49] H. S. Cho, F. Schotte, N. Dashdorj, J. Kyndt, and P. a. Anfinrud, "Probing anisotropic structure changes in proteins with picosecond time-resolved small-angle X-ray scattering.," *The journal of physical chemistry. B*, vol. 117, pp. 15825–32, 12 2013.

[50] M. Andersson, E. Malmerberg, S. Westenhoff, G. Katona, M. Cammarata, A. B. Wöhri, L. C. Johansson, F. Ewald, M. Eklund, M. Wulff, J. Davidsson, and R. Neutze, "Structural dynamics of light-driven proton pumps.," *Structure (London, England : 1993)*, vol. 17, pp. 1265–75, 9 2009.

[51] J. H. Lee, J. Kim, M. Cammarata, Q. Kong, K. H. Kim, J. Choi, T. K. Kim, M. Wulff, and H. Ihee, "Transient X-ray diffraction reveals global and major reaction pathways for the photolysis of iodoform in solution.," *Angewandte Chemie (International ed. in English)*, vol. 47, no. 6, pp. 1047–50, 2008.

[52] S. V. Kathuria, L. Guo, R. Graceffa, R. Barrea, R. P. Nobrega, C. R. Matthews, T. C. Irving, and O. Bilsel, "Minireview: Structural insights into early folding events using continuous-flow time-resolved small-angle X-ray scattering," *Biopolymers*, vol. 95, no. 8, pp. 550–558, 2011.

[53] M. Cammarata, M. Levantino, F. Schotte, P. A. Anfinrud, F. Ewald, J. Choi, A. Cupane, M. Wulff, and H. Ihee, "Tracking the structural dynamics of proteins in solution using time-resolved wide-angle X-ray scattering.," *Nature methods*, vol. 5, pp. 881–6, 10 2008.

[54] M. Andersson, J. Vincent, D. van der Spoel, J. Davidsson, and R. Neutze, "A proposed time-resolved X-ray scattering approach to track local and global conformational changes in membrane transport proteins.," *Structure (London, England : 1993)*, vol. 16, pp. 21–8, 1 2008.

[55] R. Neutze, R. Wouts, S. Techert, J. Davidsson, M. Kocsis, A. Kirrander, F. Schotte, and M. Wulff, "Visualizing photochemical dynamics in solution through picosecond x-ray scattering.," *Physical review letters*, vol. 87, p. 195508, 11 2001.

[56] A. Plech, M. Wulff, S. Bratos, F. Mirloup, R. Vuilleumier, F. Schotte, and P. A. Anfinrud, "Visualizing chemical reactions in solution by picosecond x-ray diffraction.," *Physical review letters*, vol. 92, p. 125505, 3 2004.

[57] J. Davidsson, J. Poulsen, M. Cammarata, P. Georgiou, R. Wouts, G. Katona, F. Jacobson, A. Plech, M. Wulff, G. Nyman, and R. Neutze, "Structural determination of a transient isomer of CH2I2 by picosecond X-ray diffraction," *Physical review letters*, vol. 94, no. 24, 2005.

[58] H. Ihee, "Ultrafast X-ray Diffraction of Transient Molecular Structures in Solution," *Science (New York, N.Y.)*, vol. 309, no. 5738, pp. 1223–1227, 2005.

[59] T. K. Kim, M. Lorenc, J. H. Lee, M. Lo Russo, J. Kim, M. Cammarata, Q. Kong, S. Noel, A. Plech, M. Wulff, and H. Ihee, "Spatiotemporal reaction kinetics of an ultrafast photoreaction pathway visualized by time-resolved liquid x-ray diffraction.," *Proceedings of the National Academy of Sciences of the United States of America*, vol. 103, pp. 9410–9415, 2006.

[60] P. Georgiou, J. Vincent, M. Andersson, A. B. Wöhri, P. Gourdon, J. Poulsen, J. Davidsson, and R. Neutze, "Picosecond calorimetry: time-resolved x-ray diffraction studies of liquid CH2Cl2.," *The Journal of chemical physics*, vol. 124, p. 234507, 6 2006.

[61] S. Ahn, K. H. Kim, Y. Kim, J. Kim, and H. Ihee, "Protein tertiary structural changes visualized by time-resolved X-ray solution scattering.," *The journal of physical chemistry. B*, vol. 113, pp. 13131–3, 10 2009.

[62] H. S. Cho, N. Dashdorj, F. Schotte, T. Graber, R. Henning, and P. Anfinrud, "Protein structural dynamics in solution unveiled via 100-ps time-resolved x-ray scattering.," *Proceedings of the National Academy of Sciences of the United States of America*, vol. 107, pp. 7281–6, 4 2010.

[63] S. Westenhoff, E. Malmerberg, D. Arnlund, L. Johansson, E. Nazarenko, M. Cammarata, J. Davidsson, V. Chaptal, J. Abramson, G. Katona, A. Menzel, and R. Neutze, "Rapid readout detector captures protein time-resolved WAXS.," *Nature methods*, vol. 7, pp. 775–776, 10 2010.

[64] K. H. Kim, K. Y. Oang, J. Kim, J. H. Lee, Y. Kim, and H. Ihee, "Direct observation of myoglobin structural dynamics from 100 picoseconds to 1 microsecond with picosecond X-ray solution scattering.," *Chemical communications (Cambridge, England)*, vol. 47, pp. 289–91, 1 2011.

[65] J. Kim, K. H. Kim, J. G. Kim, T. W. Kim, Y. Kim, and H. Ihee, "Anisotropic Picosecond X-ray Solution Scattering from Photo-selectively Aligned Protein Molecules.," *The journal of physical chemistry letters*, vol. 2, pp. 350–356, 2 2011.

[66] E. Malmerberg, Z. Omran, J. S. Hub, X. Li, G. Katona, S. Westenhoff, L. C. Johansson, M. Andersson, M. Cammarata, M. Wulff, D. van der Spoel, J. Davidsson, A. Specht, and R. Neutze, "Time-resolved WAXS reveals accelerated conformational changes in iodoretinal-substituted proteorhodopsin.," *Biophysical journal*, vol. 101, pp. 1345–53, 9 2011.

[67] T. W. Kim, J. H. Lee, J. Choi, K. H. Kim, L. J. van Wilderen, L. Guerin, Y. Kim, Y. O. Jung, C. Yang, J. Kim, M. Wulff, J. J. van Thor, and H. Ihee, "Protein structural dynamics of photoactive yellow protein in solution revealed by pump-probe X-ray solution scattering.," *Journal of the American Chemical Society*, vol. 134, pp. 3145–53, 2 2012.

[68] K. H. Kim, S. Muniyappan, K. Y. Oang, J. J. G. Kim, S. Nozawa, T. Sato, S.-y. Koshihara, R. Henning, I. Kosheleva, H. Ki, Y. Kim, T. W. Kim, J. J. G. Kim, S.-i. Adachi, and H. Ihee, "Direct observation of cooperative protein structural dynamics of homodimeric hemoglobin from 100 ps to 10 ms with pump-probe X-ray solution scattering.," *Journal of the American Chemical Society*, vol. 134, pp. 7001–7008, 4 2012.

[69] M. Levantino, A. Spilotros, M. Cammarata, G. Schirò, C. Ardiccioni, B. Vallone, M. Brunori, and A. Cupane, "The Monod-Wyman-Changeux allosteric model accounts for the quaternary transition dynamics in wild type and a recombinant mutant human hemoglobin.," *Proceedings of the National Academy of Sciences of the United States of America*, vol. 109, pp. 14894–14899, 9 2012.

[70] A. Spilotros, M. Levantino, G. Schirò, M. Cammarata, M. Wulff, and A. Cupane, "Probing in cell protein structural changes with time-resolved X-ray scattering," *Soft Matter*, vol. 8, no. 24, p. 6434, 2012.

[71] H. Takala, A. Björling, O. Berntsson, H. Lehtivuori, S. Niebling, M. Hoernke, I. Kosheleva, R. Henning, A. Menzel, J. A. Ihalainen, and S. Westenhoff, "Signal amplification and transduction in phytochrome photosensors.," *Nature*, vol. 509, pp. 245–8, 5 2014.

[72] K. Y. Oang, J. J. G. Kim, C. Yang, T. W. Kim, Y. Kim, K. H. Kim, J. J. G. Kim, and H. Ihee, "Conformational Substates of Myoglobin Intermediate Resolved by Picosecond X-ray Solution Scattering.," *The journal of physical chemistry letters*, vol. 5, pp. 804–808, 3 2014.

[73] D. Arnlund, L. C. Johansson, C. Wickstrand, A. Barty, G. J. Williams, E. Malmerberg, J. Davidsson, D. Milathianaki, D. P. DePonte, R. L. Shoeman, D. Wang, D. James, G. Katona, S. Westenhoff, T. A. White, A. Aquila, S. Bari, P. Berntsen, M. Bogan, T. B. van Driel, R. B. Doak, K. S. Kjær, M. Frank, R. Fromme, I. Grotjohann, R. Henning, M. S. Hunter, R. A. Kirian, I. Kosheleva, C. Kupitz, M. Liang, A. V. Martin, M. M. Nielsen, M. Messerschmidt, M. M. Seibert, J. Sjöhamn, F. Stellato, U. Weierstall, N. a. Zatsepin, J. C. H. Spence, P. Fromme, I. Schlichting, S. Boutet, G. Groenhof, H. N. Chapman, and R. Neutze, "Visualizing a protein quake with time-resolved X-ray scattering at a free-electron laser.," *Nature methods*, vol. 11, pp. 923–6, 9 2014.

[74] K. Y. Oang, K. H. Kim, J. Jo, Y. Kim, J. G. Kim, T. W. Kim, S. Jun, J. Kim, and H. Ihee, "Sub-100-ps structural dynamics of horse heart myoglobin probed by time-resolved X-ray solution scattering.," *Chemical physics*, vol. 422, pp. 137–142, 10 2014.

[75] M. Levantino, G. Schirò, H. T. Lemke, G. Cottone, J. M. Glownia, D. Zhu, M. Chollet, H. Ihee, A. Cupane, and M. Cammarata, "Ultrafast myoglobin structural dynamics observed with an X-ray free-electron laser.," *Nature communications*, vol. 6, p. 6772, 4 2015.

[76] E. Malmerberg, P. H. M Bovee-Geurts, G. Katona, X. Deupi, D. Arnlund, C. Wickstrand, L. C. Johansson, S. Westenhoff, E. Nazarenko, G. F. X. Schertler, A. Menzel, W. J. de Grip, and R. Neutze, "Conformational activation of visual rhodopsin in native disc membranes.," *Science signaling*, vol. 8, p. ra26, 3 2015.

[77] H. S. Cho, F. Schotte, N. Dashdorj, J. Kyndt, R. Henning, and P. A. Anfinrud, "Picosecond Photobiology: Watching a Signaling Protein Function in Real Time via Time-Resolved Small- and Wide-Angle X-ray Scattering," *Journal of the American Chemical Society*, vol. 138, pp. 8815–8823, 7 2016.

[78] J. J. G. Kim, S. Muniyappan, K. Y. Oang, T. W. Kim, C. Yang, K. H. Kim, J. J. G. Kim, and H. Ihee, "Cooperative protein structural dynamics of homodimeric hemoglobin linked to water cluster at subunit interface revealed by time-resolved X-ray solution scattering," *Structural Dynamics*, vol. 3, no. 2, p. 023610, 2016.

[79] J. Kim, K. H. Kim, K. Y. Oang, J. H. Lee, K. Hong, H. Cho, N. Huse, R. W. Schoenlein, T. K. Kim, and H. Ihee, "Tracking reaction dynamics in solution by pump-probe X-ray absorption spectroscopy and X-ray liquidography (solution scattering).," *Chemical communications (Cambridge, England)*, vol. 52, pp. 3734–49, 3 2016.

[80] T. W. Kim, C. Yang, Y. Kim, J. G. Kim, J. Kim, Y. O. Jung, S. Jun, S. J. Lee, S. Park, I. Kosheleva, R. Henning, J. J. van Thor, and H. Ihee, "Combined probes of X-ray scattering and optical spectroscopy reveal how global conformational change is temporally and spatially linked to local structural perturbation in photoactive yellow protein.," *Physical chemistry chemical physics : PCCP*, vol. 18, pp. 8911–8919, 4 2016.

[81] H. Takala, S. Niebling, O. Berntsson, A. Björling, H. Lehtivuori, H. Häkkänen, M. Panman, E. Gustavsson, M. Hoernke, G. Newby, F. Zontone, M. Wulff, A. Menzel, J. A. Ihalainen, and S. Westenhoff, "Light-induced structural changes in a monomeric bacteriophytochrome," *Structural Dynamics*, vol. 3, no. 5, pp. 1–12, 2016.

[82] A. Björling, O. Berntsson, H. Lehtivuori, H. Takala, A. J. Hughes, M. Panman, M. Hoernke, S. Niebling, L. Henry, R. Henning, I. Kosheleva, V. Chukharev, N. V. Tkachenko, A. Menzel, G. Newby, D. Khakhulin, M. Wulff, J. A. Ihalainen, and S. Westenhoff, "Structural photoactivation of a full-length bacterial phytochrome," *Science Advances*, vol. 2, pp. e1600920–e1600920, 8 2016.

[83] T. Graber, S. Anderson, H. Brewer, Y. S. Chen, H. S. Cho, N. Dashdorj, R. W. Henning, I. Kosheleva, G. Macha, M. Meron, R. Pahl, Z. Ren, S. Ruan, F. Schotte, V. Srajer, P. J. Viccaro, F. Westferro, P. Anfinrud, and K. Moffat, "BioCARS: a synchrotron resource for time-resolved X-ray science.," *Journal of synchrotron radiation*, vol. 18, pp. 658–70, 7 2011.

[84] B. Henrich, A. Bergamaschi, C. Broennimann, R. Dinapoli, E. F. Eikenberry, I. Johnson, M. Kobas, P. Kraft, A. Mozzanica, and B. Schmitt, "PILATUS: A single photon counting pixel detector for X-ray applications," *Nuclear Instruments and Methods in Physics Research, Section A: Accelerators, Spectrometers, Detectors and Associated Equipment*, vol. 607, no. 1, pp. 247–249, 2009.

[85] R. Dinapoli, A. Bergamaschi, B. Henrich, R. Horisberger, I. Johnson, A. Mozzanica, E. Schmid, B. Schmitt, A. Schreiber, X. Shi, and G. Theidel, "EIGER: Next generation single photon counting detector for X-ray applications," *Nuclear Instruments and Methods in Physics Research, Section A: Accelerators, Spectrometers, Detectors and Associated Equipment*, vol. 650, no. 1, pp. 79–83, 2011.

[86] K. S. Kjær, T. B. van Driel, J. Kehres, K. Haldrup, D. Khakhulin, K. Bechgaard, M. Cammarata, M. Wulff, T. J. Sørensen, and M. M. Nielsen, "Introducing a standard method for experimental determination of the solvent response in laser pump, X-ray probe time-resolved wide-angle X-ray scattering experiments on systems in solution.," *Physical chemistry chemical physics : PCCP*, vol. 15, no. 36, pp. 15003–15016, 2013.

[87] O. Carugo and K. D. Carugo, "When X-rays modify the protein structure: Radiation damage at work," *Trends in Biochemical Sciences*, vol. 30, no. 4, pp. 213–219, 2005.

[88] A. K. Røhr, H.-P. Hersleth, and K. K. Andersson, "Tracking flavin conformations in protein crystal structures with Raman spectroscopy and QM/MM calculations.," *Angewandte Chemie (International ed. in English)*, vol. 49, pp. 2324–7, 3 2010.

[89] J. C. Brooks-Bartlett, R. A. Batters, C. S. Bury, E. D. Lowe, H. M. Ginn, A. Round, and E. F. Garman, "Development of tools to automate quantitative analysis of radiation damage in SAXS experiments," *Journal of synchrotron radiation*, vol. 24, no. 1, pp. 63–72, 2017.

[90] B. R. Pauw, "Everything SAXS: small-angle scattering pattern collection and correction.," *Journal of physics. Condensed matter : an Institute of Physics journal*, vol. 25, p. 383201, 9 2013.

[91] O. Glatter, "A new method for the evaluation of small-angle scattering data," *Journal of applied crystallography*, vol. 10, pp. 415–421, 10 1977.

[92] C. E. Shannon and W. Weaver, "The Mathematical Theory of Communication," *Univ. Illinois Press*, vol. 1, p. 17, 1949.

[93] P. B. Moore, "Small-Angle Scattering. Information Content and Error Analysis," *J. Appl. Cryst.*, vol. 13, pp. 168–175, 4 1980.

[94] R. P. Rambo and J. A. Tainer, "Accurate assessment of mass, models and resolution by small-angle scattering.," *Nature*, vol. 496, pp. 477–81, 4 2013.

[95] Z. Kam, "Determination of Macromolecular Structure in Solution by Spatial Correlation of Scattering Fluctuations," *Macromolecules*, vol. 10, pp. 927–934, 9 1977.

[96] Z. Kam, M. H. Koch, and J. Bordas, "Fluctuation x-ray scattering from biological particles in frozen solution by using synchrotron radiation.," *Proceedings of the National Academy of Sciences of the United States of America*, vol. 78, pp. 3559–62, 6 1981.

[97] D. Starodub, A. Aquila, S. Bajt, M. Barthelmess, A. Barty, C. Bostedt, J. D. Bozek, N. Coppola, R. B. Doak, S. W. Epp, B. Erk, L. Foucar, L. Gumprecht, C. Y. Hampton, A. Hartmann, R. Hartmann, P. Holl, S. Kassemeyer, N. Kimmel, H. Laksmono, M. Liang, N. D. Loh, L. Lomb, a. V. Martin, K. Nass, C. Reich, D. Rolles, B. Rudek, A. Rudenko, J. Schulz, R. L. Shoeman, R. G. Sierra, H. Soltau, J. Steinbrener, F. Stellato, S. Stern, G. Weidenspointner, M. Frank, J. Ullrich, L. Strüder, I. Schlichting, H. N. Chapman, J. C. H. Spence, and M. J. Bogan, "Single-particle structure determination by correlations of snapshot X-ray diffraction patterns.," *Nature communications*, vol. 3, no. May, p. 1276, 2012.

[98] D. K. Saldin, H. C. Poon, M. J. Bogan, S. Marchesini, D. A. Shapiro, R. A. Kirian, U. Weierstall, and J. C. H. Spence, "New light on disordered ensembles: ab initio structure determination of one particle from scattering fluctuations of many copies.," *Physical review letters*, vol. 106, p. 115501, 3 2011.

[99] K. H. Kim, J. J. J. G. Kim, S. Nozawa, T. T. Sato, K. Y. Oang, T. W. Kim, H. Ki, J. Jo, S. Park, C. Song, T. T. Sato, K. Ogawa, T. Togashi, K. Tono, M. Yabashi, T. Ishikawa, J. J. J. G. Kim, R. Ryoo, J. J. J. G. Kim, H. Ihee, and S.-i. Adachi, "Direct observation of bond formation in solution with femtosecond X-ray scattering.," *Nature*, vol. 518, pp. 385–9, 2 2015.

[100] D. I. Svergun, "Determination of the Regularization Parameter in Indirect- Transform Methods Using Perceptual Criteria," *Journal of applied crystallography*, vol. 25, pp. 495–503, 1992.

[101] D. I. Svergun, "Restoring low resolution structure of biological macromolecules from solution scattering using simulated annealing.," *Biophysical journal*, vol. 76, pp. 2879–86, 6 1999.

[102] V. V. Volkov and D. I. Svergun, "Uniqueness of ab initio shape determination in small-angle scattering," *Journal of applied crystallography*, vol. 36, no. 3 I, pp. 860–864, 2003.

[103] J. G. Kim, T. W. Kim, J. Kim, and H. Ihee, "Protein structural dynamics revealed by time-resolved X-ray solution scattering.," *Accounts of chemical research*, vol. 48, pp. 2200–8, 8 2015.

[104] M. J. Abraham, T. Murtola, R. Schulz, S. Páll, J. C. Smith, B. Hess, and E. Lindahl, "GROMACS: High performance molecular simulations through multi-level parallelism from laptops to supercomputers," *SoftwareX*, vol. 1-2, pp. 19–25, 9 2015.

[105] T. Maximova, R. Moffatt, B. Ma, R. Nussinov, and A. Shehu, "Principles and Overview of Sampling Methods for Modeling Macromolecular Structure and Dynamics.," *PLoS computational biology*, vol. 12, p. e1004619, 4 2016.

[106] L. E. Spardy, S. N. Markin, N. A. Shevtsova, B. I. Prilutsky, I. A. Rybak, and J. E. Rubin, "A dynamical systems analysis of afferent control in a neuromechanical model of locomotion: II. Phase asymmetry," *Journal of Neural Engineering*, vol. 8, p. 065004, 10 2011.

[107] L. Zhang, S. Bouguet-Bonnet, and M. Buck, "Combining NMR and molecular dynamics studies for insights into the allostery of small GTPase-protein interactions.," *Methods in molecular biology (Clifton, N.J.)*, vol. 796, no. 2, pp. 235–59, 2012.

[108] A. Björling, S. Niebling, M. Marcellini, D. van der Spoel, and S. Westenhoff, "Deciphering Solution Scattering Data with Experimentally Guided Molecular Dynamics Simulations," *Journal of chemical theory and computation*, vol. 11, no. 2, pp. 780–787, 2015.

[109] A. Björling, *Detecting and Identifying Solution-structural Change in Photoactive Proteins*. PhD thesis, 2015.

[110] M. E. Auldridge and K. T. Forest, "Bacterial phytochromes: more than meets the light.," *Critical reviews in biochemistry and molecular biology*, vol. 46, pp. 67–88, 2 2011.

[111] R. E. Kendrick and C. J. Spruit, "Phototransformations of phytochrome.," *Photochemistry and photobiology*, vol. 26, pp. 201–14, 8 1977.

[112] N. C. Rockwell, Y.-S. Su, and J. C. Lagarias, "Phytochrome structure and signaling mechanisms.," *Annual review of plant biology*, vol. 57, no. 1, pp. 837–58, 2006.

[113] B. Karniol and R. D. Vierstra, "The pair of bacteriophytochromes from Agrobacterium tumefaciens are histidine kinases with opposing photobiological properties.," *Proceedings of the National Academy of Sciences of the United States of America*, vol. 100, pp. 2807–12, 3 2003.

[114] J. R. Wagner, J. S. Brunzelle, K. T. Forest, and R. D. Vierstra, "A light-sensing knot revealed by the structure of the chromophore-binding domain of phytochrome.," *Nature*, vol. 438, pp. 325–31, 11 2005.

[115] L.-O. Essen, J. Mailliet, and J. Hughes, "The structure of a complete phytochrome sensory module in the Pr ground state.," *Proceedings of the National Academy of Sciences of the United States of America*, vol. 105, pp. 14709–14, 9 2008.

[116] X. Yang, J. Kuk, and K. Moffat, "Crystal structure of Pseudomonas aeruginosa bacteriophytochrome: photoconversion and signal transduction.," *Proceedings of the National Academy of Sciences of the United States of America*, vol. 105, pp. 14715–20, 9 2008.

[117] D. Bellini and M. Z. Papiz, "Structure of a bacteriophytochrome and light-stimulated protomer swapping with a gene repressor.," *Structure (London, England : 1993)*, vol. 20, pp. 1436–46, 8 2012.

[118] K. Anders, G. Daminelli-Widany, M. A. Mroginski, D. von Stetten, and L.-O. Essen, "Structure of the cyanobacterial phytochrome 2 photosensor implies a tryptophan switch for phytochrome signaling.," *The Journal of biological chemistry*, vol. 288, pp. 35714–25, 12 2013.

[119] E. S. Burgie, A. N. Bussell, J. M. Walker, K. Dubiel, and R. D. Vierstra, "Crystal structure of the photosensing module from a red/far-red light-absorbing plant phytochrome.," *Proceedings of the National Academy of Sciences of the United States of America*, vol. 111, pp. 10179–84, 7 2014.

[120] C. Song, G. Psakis, C. Lang, J. Mailliet, W. Gärtner, J. Hughes, and J. Matysik, "Two ground state isoforms and a chromophore D-ring photoflip triggering extensive intramolecular changes in a canonical phytochrome.," *Proceedings of the National Academy of Sciences of the United States of America*, vol. 108, pp. 3842–7, 3 2011.

[121] E. S. Burgie, J. Zhang, and R. D. Vierstra, "Crystal Structure of Deinococcus Phytochrome in the Photoactivated State Reveals a Cascade of Structural Rearrangements during Photoconversion.," *Structure (London, England : 1993)*, vol. 24, pp. 448–457, 3 2016.

[122] A. Möglich and K. Moffat, "Engineered photoreceptors as novel optogenetic tools.," *Photochemical & photobiological sciences : Official journal of the European Photochemistry Association and the European Society for Photobiology*, vol. 9, pp. 1286–300, 10 2010.

[123] S. H. Bhoo, S. J. Davis, J. Walker, B. Karniol, and R. D. Vierstra, "Bacteriophytochromes are photochromic histidine kinases using a biliverdin chromophore.," *Nature*, vol. 414, pp. 776–9, 12 2001.

[124] K. C. Yeh and J. C. Lagarias, "Eukaryotic phytochromes: light-regulated serine/threonine protein kinases with histidine kinase ancestry.," *Proceedings of the National Academy of Sciences of the United States of America*, vol. 95, pp. 13976–81, 11 1998.

[125] K. A. Franklin and P. H. Quail, "Phytochrome functions in Arabidopsis development.," *Journal of experimental botany*, vol. 61, no. 1, pp. 11–24, 2010.

[126] J. Hughes, "Phytochrome cytoplasmic signaling.," *Annual review of plant biology*, vol. 64, pp. 377–402, 2013.

[127] G. Bae and G. Choi, "Decoding of light signals by plant phytochromes and their interacting proteins.," *Annual review of plant biology*, vol. 59, pp. 281–311, 2008.

[128] B. Borucki, D. von Stetten, S. Seibeck, T. Lamparter, N. Michael, M. A. Mroginski, H. Otto, D. H. Murgida, M. P. Heyn, and P. Hildebrandt, "Light-induced proton release of phytochrome is coupled to the transient deprotonation of the tetrapyrrole chromophore.," *The Journal of biological chemistry*, vol. 280, pp. 34358–64, 10 2005.

[129] B. Borucki, S. Seibeck, M. P. Heyn, and T. Lamparter, "Characterization of the covalent and noncovalent adducts of Agp1 phytochrome assembled with biliverdin and phycocyanobilin by circular dichroism and flash photolysis.," *Biochemistry*, vol. 48, pp. 6305–17, 7 2009.

[130] A. Remberg, I. Lindner, T. Lamparter, J. Hughes, C. Kneip, P. Hildebrandt, S. E. Braslavsky, W. Gärtner, and K. Schaffner, "Raman spectroscopic and light-induced kinetic characterization of a recombinant phytochrome of the cyanobacterium Synechocystis.," *Biochemistry*, vol. 36, pp. 13389–95, 10 1997.

[131] J. J. van Thor, B. Borucki, W. Crielaard, H. Otto, T. Lamparter, J. Hughes, K. J. Hellingwerf, and M. P. Heyn, "Light-induced proton release and proton uptake reactions in the cyanobacterial phytochrome Cph1.," *Biochemistry*, vol. 40, pp. 11460–71, 9 2001.

[132] H. Linschitz and V. Kasche, "The kinetics of phytochrome conversion.," *The Journal of biological chemistry*, vol. 241, pp. 3395–403, 7 1966.

[133] P. F. Aramendia, B. L. P. Ruzsicska, S. E. BraSlavsky, and K. Schaffner, "Laser flash photolysis of 124-kilodalton oat phytochrome in H 2 O and D 2 O solutions: formation and decay of the I 700 intermediates.," *Biochemistry*, vol. 26, no. 5, pp. 1418–1422, 1987.

[134] P. Schmidt, T. Gertsch, A. Remberg, W. Gärtner, S. E. Braslavsky, and K. Schaffner, "The Complexity of the P r to P fr Phototransformation Kinetics Is an Intrinsic Property of Native Phytochrome*," *Photochemistry and photobiology*, vol. 68, pp. 754–761, 11 1998.

[135] U. Robben, I. Lindner, and W. Gärtner, "New open-chain tetrapyrroles as chromophores in the plant photoreceptor phytochrome.," *Journal of the American Chemical Society*, vol. 130, pp. 11303–11, 8 2008.

[136] M. A. Mroginski, D. H. Murgida, and P. Hildebrandt, "The chromophore structural changes during the photocycle of phytochrome: a combined resonance Raman and quantum chemical approach.," *Accounts of chemical research*, vol. 40, pp. 258–66, 4 2007.

[137] P. Edlund, H. Takala, E. Claesson, L. Henry, R. Dods, H. Lehtivuori, M. Panman, K. Pande, T. White, T. Nakane, O. Berntsson, E. Gustavsson, P. Båth, V. Modi, S. Roy-Chowdhury, J. Zook, P. Berntsen, S. Pandey, I. Poudyal, J. Tenboer, C. Kupitz, A. Barty, P. Fromme, J. D. Koralek, T. Tanaka, J. Spence, M. Liang, M. S. Hunter, S. Boutet, E. Nango, K. Moffat, G. Groenhof, J. Ihalainen, E. A. Stojković, M. Schmidt, and S. Westenhoff, "The room temperature crystal structure of a bacterial phytochrome determined by serial femtosecond crystallography.," *Scientific reports*, vol. 6, p. 35279, 10 2016.

[138] E. A. Stojković, K. C. Toh, M. T. A. Alexandre, M. Baclayon, K. Moffat, and J. T. M. Kennis, "FTIR Spectroscopy Revealing Light-Dependent Refolding of the Conserved Tongue Region of Bacteriophytochrome.," *The journal of physical chemistry letters*, vol. 5, pp. 2512–2515, 8 2014.

[139] F. Velazquez Escobar, P. Piwowarski, J. Salewski, N. Michael, M. Fernandez Lopez, A. Rupp, B. M. Qureshi, P. Scheerer, F. Bartl, N. Frankenberg-Dinkel, F. Siebert, M. Andrea Mroginski, and P. Hildebrandt, "A protonation-coupled feedback mechanism controls the signalling process in bathy phytochromes.," *Nature chemistry*, vol. 7, pp. 423–30, 5 2015.

[140] K. Anders, A. Gutt, W. Gärtner, and L.-O. Essen, "Phototransformation of the red light sensor cyanobacterial phytochrome 2 from Synechocystis species depends on its tongue motifs.," *The Journal of biological chemistry*, vol. 289, pp. 25590–600, 9 2014.

[141] A. Björling, O. Berntsson, H. Takala, K. D. Gallagher, H. Patel, E. Gustavsson, R. St Peter, P. Duong, A. Nugent, F. Zhang, P. Berntsen, R. Appio, I. Rajkovic, H. Lehtivuori, M. R. Panman, M. Hoernke, S. Niebling, R. Harimoorthy, T. Lamparter, E. A. Stojković, J. A. Ihalainen, and S. Westenhoff, "Ubiquitous Structural Signaling in Bacterial Phytochromes.," *The journal of physical chemistry letters*, vol. 6, pp. 3379–83, 9 2015.

[142] T. Mathes, J. Ravensbergen, M. Kloz, T. Gleichmann, K. D. Gallagher, N. C. Woitowich, R. St Peter, S. E. Kovaleva, E. A. Stojković, and J. T. M. Kennis, "Femto- to Microsecond Photodynamics of an Unusual Bacteriophytochrome.," *The journal of physical chemistry letters*, vol. 6, pp. 239–43, 1 2015.

[143] H. Li, J. Zhang, R. D. Vierstra, and H. Li, "Quaternary organization of a phytochrome dimer as revealed by cryoelectron microscopy.," *Proceedings of the National Academy of Sciences of the United States of America*, vol. 107, pp. 10872–7, 6 2010.

[144] E. S. Burgie, T. Wang, A. N. Bussell, J. M. Walker, H. Li, and R. D. Vierstra, "Crystallographic and electron microscopic analyses of a bacterial phytochrome reveal local and global rearrangements during photoconversion.," *The Journal of biological chemistry*, vol. 289, pp. 24573–87, 8 2014.

[145] H. Takala, A. Björling, M. Linna, S. Westenhoff, and J. A. Ihalainen, "Light-induced Changes in the Dimerization Interface of Bacteriophytochromes.," *The Journal of biological chemistry*, vol. 290, pp. 16383–92, 6 2015.

[146] M. P. Bhate, K. S. Molnar, M. Goulian, and W. F. DeGrado, "Signal transduction in histidine kinases: insights from new structures.," *Structure (London, England : 1993)*, vol. 23, pp. 981–94, 6 2015.

[147] S. Kacprzak, I. Njimona, A. Renz, J. Feng, E. Reijerse, W. Lubitz, N. Krauss, P. Scheerer, S. Nagano, T. Lamparter, and S. Weber, "Intersubunit distances in full-length, dimeric, bacterial phytochrome Agp1, as measured by pulsed electron-electron double resonance (PELDOR) between different spin label positions, remain unchanged upon photoconversion.," *The Journal of biological chemistry*, vol. 292, pp. 7598–7606, 5 2017.

[148] A. E. Dago, A. Schug, A. Procaccini, J. A. Hoch, M. Weigt, and H. Szurmant, "Structural basis of histidine kinase autophosphorylation deduced by integrating genomics, molecular dynamics, and mutagenesis.," *Proceedings of the National Academy of Sciences of the United States of America*, vol. 109, pp. 1733–42, 6 2012.

[149] K. S. Conrad, C. C. Manahan, and B. R. Crane, "Photochemistry of flavoprotein light sensors," *Nature Chemical Biology*, vol. 10, pp. 801–809, 9 2014.

[150] P. Ballario, P. Vittorioso, A. Magrelli, C. Talora, A. Cabibbo, and G. Macino, "White collar-1, a central regulator of blue light responses in Neurospora, is a zinc finger protein.," *The EMBO journal*, vol. 15, pp. 1650–1657, 4 1996.

[151] M. Avila-Pérez, K. J. Hellingwerf, and R. Kort, "Blue light activates the sigmaB-dependent stress response of Bacillus subtilis via YtvA.," *Journal of bacteriology*, vol. 188, pp. 6411–6414, 9 2006.

[152] T. A. Gaidenko, T.-J. Kim, A. L. Weigel, M. S. Brody, and C. W. Price, "The blue-light receptor YtvA acts in the environmental stress signaling pathway of Bacillus subtilis.," *Journal of bacteriology*, vol. 188, pp. 6387–6395, 9 2006.

[153] S. T. Glantz, E. J. Carpenter, M. Melkonian, K. H. Gardner, E. S. Boyden, G. K.-S. Wong, and B. Y. Chow, "Functional and topological diversity of LOV domain photoreceptors.," *Proceedings of the National Academy of Sciences of the United States of America*, vol. 113, pp. 1442–51, 3 2016.

[154] Y. I. Wu, D. Frey, O. I. Lungu, A. Jaehrig, I. Schlichting, B. Kuhlman, and K. M. Hahn, "A genetically encoded photoactivatable Rac controls the motility of living cells.," *Nature*, vol. 461, pp. 104–108, 9 2009.

[155] S. Crosson and K. Moffat, "Structure of a flavin-binding plant photoreceptor domain: insights into light-mediated signal transduction.," *Proceedings of the National Academy of Sciences of the United States of America*, vol. 98, pp. 2995–3000, 3 2001.

[156] J. M. Christie, M. Salomon, K. Nozue, M. Wada, and W. R. Briggs, "LOV (light, oxygen, or voltage) domains of the blue-light photoreceptor phototropin (nph1): binding sites for the chromophore flavin mononucleotide.," *Proceedings of the National Academy of Sciences of the United States of America*, vol. 96, pp. 8779–83, 7 1999.

[157] J. Herrou and S. Crosson, "Function, structure and mechanism of bacterial photosensory LOV proteins.," *Nature reviews. Microbiology*, vol. 9, pp. 713–23, 8 2011.

[158] B. D. Zoltowski and K. H. Gardner, "Tripping the light fantastic: blue-light photoreceptors as examples of environmentally modulated protein-protein interactions.," *Biochemistry*, vol. 50, pp. 4–16, 1 2011.

[159] J. T. M. Kennis, S. Crosson, M. Gauden, I. H. M. van Stokkum, K. Moffat, and R. van Grondelle, "Primary reactions of the LOV2 domain of phototropin, a plant blue-light photoreceptor.," *Biochemistry*, vol. 42, pp. 3385–92, 4 2003.

[160] T. E. Swartz, S. B. Corchnoy, J. M. Christie, J. W. Lewis, I. Szundi, W. R. Briggs, and R. a. Bogomolni, "The photocycle of a flavin-binding domain of the blue light photoreceptor phototropin.," *The Journal of biological chemistry*, vol. 276, pp. 36493–500, 9 2001.

[161] M. Salomon, J. M. Christie, E. Knieb, U. Lempert, and W. R. Briggs, "Photochemical and mutational analysis of the FMN-binding domains of the plant blue light receptor, phototropin.," *Biochemistry*, vol. 39, pp. 9401–9410, 8 2000.

[162] E. F. Yee, R. P. Diensthuber, A. T. Vaidya, P. P. Borbat, C. Engelhard, J. H. Freed, R. Bittl, A. Möglich, and B. R. Crane, "Signal transduction in light-oxygen-voltage receptors lacking the adduct-forming cysteine residue.," *Nature communications*, vol. 6, p. 10079, 12 2015.

[163] S. Crosson and K. Moffat, "Photoexcited structure of a plant photoreceptor domain reveals a light-driven molecular switch.," *The Plant cell*, vol. 14, pp. 1067–75, 5 2002.

[164] A. Möglich and K. Moffat, "Structural basis for light-dependent signaling in the dimeric LOV domain of the photosensor YtvA.," *Journal of molecular biology*, vol. 373, pp. 112–26, 10 2007.

[165] B. D. Zoltowski, C. Schwerdtfeger, J. Widom, J. J. Loros, A. M. Bilwes, J. C. Dunlap, and B. R. Crane, "Conformational switching in the fungal light sensor Vivid.," *Science (New York, N.Y.)*, vol. 316, pp. 1054–7, 5 2007.

[166] T. Iwata, D. Nozaki, S. Tokutomi, and H. Kandori, "Comparative investigation of the LOV1 and LOV2 domains in Adiantum phytochrome3.," *Biochemistry*, vol. 44, pp. 7427–7434, 5 2005.

[167] M. T. A. Alexandre, R. van Grondelle, K. J. Hellingwerf, and J. T. M. Kennis, "Conformational heterogeneity and propagation of structural changes in the LOV2/Jalpha domain from Avena sativa phototropin 1 as recorded by temperature-dependent FTIR spectroscopy.," *Biophysical journal*, vol. 97, pp. 238–247, 7 2009.

[168] A. T. Vaidya, C.-H. Chen, J. C. Dunlap, J. J. Loros, and B. R. Crane, "Structure of a light-activated LOV protein dimer that regulates transcription.," *Science signaling*, vol. 4, p. ra50, 8 2011.

[169] K. S. Conrad, A. M. Bilwes, and B. R. Crane, "Light-induced subunit dissociation by a light-oxygen-voltage domain photoreceptor from Rhodobacter sphaeroides.," *Biochemistry*, vol. 52, pp. 378–391, 1 2013.

[170] U. Heintz and I. Schlichting, "Blue light-induced LOV domain dimerization enhances the affinity of Aureochrome 1a for its target DNA sequence.," *eLife*, vol. 5, p. e11860, 1 2016.

[171] S. M. Harper, L. C. Neil, and K. H. Gardner, "Structural basis of a phototropin light switch.," *Science (New York, N.Y.)*, vol. 301, pp. 1541–4, 9 2003.

[172] A. Möglich, R. A. Ayers, and K. Moffat, "Design and signaling mechanism of light-regulated histidine kinases.," *Journal of molecular biology*, vol. 385, pp. 1433–44, 2 2009.

[173] A. Losi, E. Polverini, B. Quest, and W. Gärtner, "First evidence for phototropin-related blue-light receptors in prokaryotes.," *Biophysical journal*, vol. 82, pp. 2627–34, 5 2002.

[174] C. Engelhard, R. P. Diensthuber, A. Möglich, and R. Bittl, "Blue-light reception through quaternary transitions.," *Scientific reports*, vol. 7, p. 1385, 5 2017.

[175] E. Saita, L. A. Abriata, Y. T. Tsai, F. Trajtenberg, T. Lemmin, A. Buschiazzo, M. Dal Peraro, D. de Mendoza, and D. Albanesi, "A coiled coil switch mediates cold sensing by the thermosensory protein DesK.," *Molecular microbiology*, vol. 98, pp. 258–71, 10 2015.

[176] S. Matamouros, K. R. Hager, and S. I. Miller, "HAMP Domain Rotation and Tilting Movements Associated with Signal Transduction in the PhoQ Sensor Kinase.," *mBio*, vol. 6, pp. 00616–15, 5 2015.

[177] R. Ohlendorf, C. H. Schumacher, F. Richter, and A. Möglich, "Library-Aided Probing of Linker Determinants in Hybrid Photoreceptors.," *ACS synthetic biology*, vol. 5, pp. 1117–1126, 10 2016.

[178] G. Rivera-Cancel, W.-h. Ko, D. R. Tomchick, F. Correa, and K. H. Gardner, "Full-length structure of a monomeric histidine kinase reveals basis for sensory regulation.," *Proceedings of the National Academy of Sciences of the United States of America*, vol. 111, pp. 17839–44, 12 2014.

[179] R. D. Finn, P. Coggill, R. Y. Eberhardt, S. R. Eddy, J. Mistry, A. L. Mitchell, S. C. Potter, M. Punta, M. Qureshi, A. Sangrador-Vegas, G. A. Salazar, J. Tate, and A. Bateman, "The Pfam protein families database: towards a more sustainable future.," *Nucleic acids research*, vol. 44, pp. 279–285, 1 2016.

[180] M. Ahmad and A. R. Cashmore, "HY4 gene of A. thaliana encodes a protein with characteristics of a blue-light photoreceptor.," *Nature*, vol. 366, pp. 162–6, 11 1993.

[181] I. Chaves, R. Pokorny, M. Byrdin, N. Hoang, T. Ritz, K. Brettel, L.-O. Essen, G. T. J. van der Horst, A. Batschauer, and M. Ahmad, "The cryptochromes: blue light photoreceptors in plants and animals.," *Annual review of plant biology*, vol. 62, pp. 335–364, 2011.

[182] K. Brettel and M. Byrdin, "Reaction mechanisms of DNA photolyase.," *Current opinion in structural biology*, vol. 20, pp. 693–701, 12 2010.

[183] P. Emery, W. V. So, M. Kaneko, J. C. Hall, and M. Rosbash, "CRY, a Drosophila clock and light-regulated cryptochrome, is a major contributor to circadian rhythm resetting and photosensitivity.," *Cell*, vol. 95, pp. 669–679, 11 1998.

[184] R. Stanewsky, M. Kaneko, P. Emery, B. Beretta, K. Wager-Smith, S. A. Kay, M. Rosbash, and J. C. Hall, "The cryb mutation identifies cryptochrome as a circadian photoreceptor in Drosophila.," *Cell*, vol. 95, pp. 681–92, 11 1998.

[185] C. A. Dodson, P. J. Hore, and M. I. Wallace, "A radical sense of direction: signalling and mechanism in cryptochrome magnetoreception.," *Trends in biochemical sciences*, vol. 38, pp. 435–446, 9 2013.

[186] M. F. Ceriani, T. K. Darlington, D. Staknis, P. Más, A. A. Petti, C. J. Weitz, and S. A. Kay, "Light-dependent sequestration of TIMELESS by CRYPTOCHROME.," *Science (New York, N.Y.)*, vol. 285, pp. 553–6, 7 1999.

[187] B. R. Crane and M. W. Young, "Interactive features of proteins composing eukaryotic circadian clocks.," *Annual review of biochemistry*, vol. 83, no. 1, pp. 191–219, 2014.

[188] R. Brudler, K. Hitomi, H. Daiyasu, H. Toh, K. I. Kucho, M. Ishiura, M. Kanehisa, V. A. Roberts, T. Todo, J. A. Tainer, and E. D. Getzoff, "Identification of a new cryptochrome class: Structure, function, and evolution," *Molecular Cell*, vol. 11, no. 1, pp. 59–67, 2003.

[189] C. A. Brautigam, B. S. Smith, Z. Ma, M. Palnitkar, D. R. Tomchick, M. Machius, and J. Deisenhofer, "Structure of the photolyase-like domain of cryptochrome 1 from Arabidopsis thaliana.," *Proceedings of the National Academy of Sciences of the United States of America*, vol. 101, pp. 12142–7, 8 2004.

[190] A. Sancar, "Structure and function of DNA photolyase.," *Biochemistry*, vol. 33, pp. 2–9, 1 1994.

[191] T. Klar, R. Pokorny, J. Moldt, A. Batschauer, and L. O. Essen, "Cryptochrome 3 from Arabidopsis thaliana: Structural and Functional Analysis of its Complex with a Folate Light Antenna," *Journal of Molecular Biology*, vol. 366, no. 3, pp. 954–964, 2007.

[192] B. D. Zoltowski, A. T. Vaidya, D. Top, J. Widom, M. W. Young, and B. R. Crane, "Structure of full-length Drosophila cryptochrome.," *Nature*, vol. 480, pp. 396–9, 11 2011.

[193] M. J. Maul, T. R. M. Barends, A. F. Glas, M. J. Cryle, T. Domratcheva, S. Schneider, I. Schlichting, and T. Carell, "Crystal structure and mechanism of a DNA (6-4) photolyase.," *Angewandte Chemie (International ed. in English)*, vol. 47, no. 52, pp. 10076–80, 2008.

[194] A. Czarna, A. Berndt, H. R. Singh, A. Grudziecki, A. G. Ladurner, G. Timinszky, A. Kramer, and E. Wolf, "Structures of Drosophila cryptochrome and mouse cryptochrome1 provide insight into circadian function.," *Cell*, vol. 153, pp. 1394–405, 6 2013.

[195] C. Levy, B. D. Zoltowski, A. R. Jones, A. T. Vaidya, D. Top, J. Widom, M. W. Young, N. S. Scrutton, B. R. Crane, and D. Leys, "Updated structure of Drosophila cryptochrome.," *Nature*, vol. 495, pp. 3–4, 3 2013.

[196] A. Berndt, T. Kottke, H. Breitkreuz, R. Dvorsky, S. Hennig, M. Alexander, and E. Wolf, "A novel photoreaction mechanism for the circadian blue light photoreceptor Drosophila cryptochrome.," *The Journal of biological chemistry*, vol. 282, pp. 13011–21, 4 2007.

[197] N. Ozturk, C. P. Selby, Y. Annayev, D. Zhong, and A. Sancar, "Reaction mechanism of Drosophila cryptochrome.," *Proceedings of the National Academy of Sciences of the United States of America*, vol. 108, pp. 516–21, 1 2011.

[198] A. Ganguly, C. C. Manahan, D. Top, E. F. Yee, C. Lin, M. W. Young, W. Thiel, and B. R. Crane, "Changes in active site histidine hydrogen bonding trigger cryptochrome activation.," *Proceedings of the National Academy of Sciences of the United States of America*, vol. 113, pp. 10073–8, 9 2016.

[199] D. Nohr, S. Franz, R. Rodriguez, B. Paulus, L.-O. Essen, S. Weber, and E. Schleicher, "Extended Electron-Transfer in Animal Cryptochromes Mediated by a Tetrad of Aromatic Amino Acids.," *Biophysical journal*, vol. 111, pp. 301–11, 7 2016.

[200] P. Müller, J. Yamamoto, R. Martin, S. Iwai, and K. Brettel, "Discovery and functional analysis of a 4th electron-transferring tryptophan conserved exclusively in animal cryptochromes and (6-4) photolyases.," *Chemical communications (Cambridge, England)*, vol. 51, pp. 15502–5, 11 2015.

[201] B. Paulus, C. Bajzath, F. Melin, L. Heidinger, V. Kromm, C. Herkersdorf, U. Benz, L. Mann, P. Stehle, P. Hellwig, S. Weber, and E. Schleicher, "Spectroscopic characterization of radicals and radical pairs in fruit fly cryptochrome - protonated and nonprotonated flavin radical-states.," *The FEBS journal*, vol. 282, pp. 3175–89, 8 2015.

[202] A. T. Vaidya, D. Top, C. C. Manahan, J. M. Tokuda, S. Zhang, L. Pollack, M. W. Young, and B. R. Crane, "Flavin reduction activates Drosophila cryptochrome.," *Proceedings of the National Academy of Sciences of the United States of America*, vol. 110, pp. 20455–60, 12 2013.

[203] M. Kondoh, C. Shiraishi, P. Müller, M. Ahmad, K. Hitomi, E. D. Getzoff, and M. Terazima, "Light-induced conformational changes in full-length Arabidopsis thaliana cryptochrome.," *Journal of molecular biology*, vol. 413, pp. 128–37, 10 2011.

[204] K. Hitomi, H. Nakamura, S. T. Kim, T. Mizukoshi, T. Ishikawa, S. Iwai, and T. Todo, "Role of two histidines in the (6-4) photolyase reaction.," *The Journal of biological chemistry*, vol. 276, pp. 10103–9, 3 2001.

[205] E. Schleicher, K. Hitomi, C. W. M. Kay, E. D. Getzoff, T. Todo, and S. Weber, "Electron nuclear double resonance differentiates complementary roles for active site histidines in (6-4) photolyase.," *The Journal of biological chemistry*, vol. 282, pp. 4738–47, 2 2007.

[206] D. Yamada, T. Iwata, J. Yamamoto, K. Hitomi, T. Todo, S. Iwai, E. D. Getzoff, and H. Kandori, "Structural role of two histidines in the (6-4) photolyase reaction.," *Biophysics and physicobiology*, vol. 12, pp. 139–44, 2015.

[207] D. Kimanius, I. Pettersson, G. Schluckebier, E. Lindahl, and M. Andersson, "SAXS-Guided Metadynamics," *Journal of chemical theory and computation*, vol. 11, pp. 3491–3498, 7 2015.

[208] L. U. L. Brinkmann and J. S. Hub, "Ultrafast anisotropic protein quake propagation after CO photodissociation in myoglobin.," *Proceedings of the National Academy of Sciences of the United States of America*, vol. 113, pp. 10565–70, 9 2016.

[209] M. Levantino, B. A. Yorke, D. C. Monteiro, M. Cammarata, and A. R. Pearson, "Using synchrotrons and XFELs for time-resolved X-ray crystallography and solution scattering experiments on biomolecules.," *Current opinion in structural biology*, vol. 35, pp. 41–8, 12 2015.

[210] D. Rimmerman, D. Leshchev, D. J. Hsu, J. Hong, I. Kosheleva, and L. X. Chen, "Direct Observation of Insulin Association Dynamics with Time-Resolved X-ray Scattering.," *The journal of physical chemistry letters*, pp. 4413–4418, 9 2017.

[211] I. V. Lundholm, H. Rodilla, W. Y. Wahlgren, A. Duelli, G. Bourenkov, J. Vukusic, R. Friedman, J. Stake, T. Schneider, and G. Katona, "Terahertz radiation induces non-thermal structural changes associated with Fröhlich condensation in a protein crystal.," *Structural dynamics (Melville, N.Y.)*, vol. 2, p. 054702, 9 2015.

[212] D. R. Hekstra, K. I. White, M. A. Socolich, R. W. Henning, V. Šrajer, and R. Ranganathan, "Electric-field-stimulated protein mechanics.," *Nature*, vol. 540, no. 7633, pp. 400–405, 2016.